

# THE SIGNIFICANCE OF THE CONFIGURATION SPACE LIE GROUP FOR THE CONSTRAINT SATISFACTION IN NUMERICAL TIME INTEGRATION OF MULTIBODY SYSTEMS

Andreas Müller

University of Michigan - Shanghai Jiao Tong University Joint Institute,  
Shanghai, China, andreas.mueller@ieee.org

Zdravko Terze

Faculty of Mechanical Engineering and Naval Architecture  
University of Zagreb, Croatia, zdravko.terze@fsb.hr

## ABSTRACT

The dynamics simulation of multibody systems (MBS) using spatial velocities (non-holonomic velocities) requires time integration of the dynamics equations together with the kinematic reconstruction equations (relating time derivatives of configuration variables to rigid body velocities). The latter are specific to the geometry of the rigid body motion underlying a particular formulation, and thus to the used configuration space (c-space). The proper c-space of a rigid body is the Lie group  $SE(3)$ , and the geometry is that of the screw motions. The rigid bodies within a MBS are further subjected to geometric constraints, often due to lower kinematic pairs that define  $SE(3)$  subgroups. Traditionally, however, in MBS dynamics the translations and rotations are parameterized independently, which implies the use of the direct product group  $SO(3) \times \mathbb{R}^3$  as rigid body c-space, although this does not account for rigid body motions. Hence, its appropriateness was recently put into perspective.

In this paper the significance of the c-space for the constraint satisfaction in numerical time stepping schemes is analyzed for holonomically constrained MBS modeled with the 'absolute coordinate' approach, i.e. using the Newton-Euler equations for the individual bodies subjected to geometric constraints. The numerical problem is considered from the kinematic perspective. It is shown that the geometric constraints a body is subjected to are exactly satisfied if they constrain the motion to a subgroup of its c-space. Since only the  $SE(3)$  subgroups have a practical significance it is regarded as the appropriate c-space for the constrained rigid body. Consequently the constraints imposed by lower pair joints are exactly satisfied if the joint connects a body to the ground. For a general MBS, where the motions are not constrained to a subgroup, the  $SE(3)$  and  $SO(3) \times \mathbb{R}^3$  yield the same order of accuracy. Hence an appropriate configuration update can be selected for each individual body of a particular MBS, which gives rise to tailored update schemes. Several numerical examples are reported illustrating this statement.

The practical consequence of using  $SE(3)$  is the use of screw coordinates as generalized coordinates. To account for the inevitable singularities of 3-parametric descriptions of rotations, the kinematic reconstruction is additionally formulated in terms of (dependent) dual quaternions as well as a coordinate-free ODE on the c-space Lie group. The latter can be solved numerically with Lie group integrators like the Munthe-Kaas integration method, which is recalled in this paper.

*Keywords*– Numerical time integration, differential algebraic equations (DAE), multibody dynamics, absolute coordinate formulation, constraints, rigid body kinematics, screws, Lie groups, isotropy groups, configuration space, SE(3)

## 1 Introduction

The seemingly simple problem addressed in this paper is how to numerically reconstruct the finite motion of a constrained rigid body within a MBS from its velocity field so that the overall system of geometric constraints is satisfied. When a rigid body moves it performs a translation together with a rotation since a general rigid body motion is a screw motion, with coupled rotation and translation. Even though standard numerical integration schemes for MBS neglect the geometry of Euclidean motion in the sense that, within the integration schemes, the position and orientation updates are performed independently. Whether or not their dependence is respected has to do with the geometric model used to represent rigid body motions, i.e. with the configuration space (c-space) Lie group. It is known that rigid body motions form the Lie group  $SE(3)$  [53, 62].

With the 'absolute coordinate' formalism (i.e. representing the spatial configuration of each body by a set of six generalized coordinates) the equations governing the dynamics of a constrained MBS comprising  $n$  rigid bodies are commonly written in the form

$$\mathbf{M}(\mathbf{q}) \dot{\mathbf{V}} + \mathbf{J}^T \boldsymbol{\lambda} = \mathbf{Q}(\mathbf{q}, \mathbf{V}, t) \quad a) \quad (1)$$

$$\mathbf{V} = \mathbf{A}(\mathbf{q}) \dot{\mathbf{q}} \quad b) \quad (1)$$

$$\mathbf{h}(\mathbf{q}) = \mathbf{0}. \quad c) \quad (1)$$

The  $N = 6n$  dimensional coordinates vector  $\mathbf{q} = (\boldsymbol{\theta}_i, \mathbf{r}_i) \in \mathbb{V}^N$  comprises the position vector  $\mathbf{r}_i$  and the vector  $\boldsymbol{\theta}_i$  consisting of 3 (or 4 dependent) rotation parameters for body  $i = 1, \dots, n$ , and  $\mathbf{V} = (\boldsymbol{\omega}_i, \mathbf{v}_i) \in \mathbb{R}^N$  is composed of the angular and linear velocity vectors  $\boldsymbol{\omega}_i$  and  $\mathbf{v}_i$ , respectively. The matrix  $\mathbf{J}$  is the constraint Jacobian corresponding to the system (1c) of geometric constraints.

The equations (1) constitute a DAE system on the coordinate manifold  $\mathbb{V}^N$  considered as vector space. From a kinematic point of view this formulation raises two issues regarding their numerical solution:

1. The motion of the MBS is deduced from the velocity  $\mathbf{V}$  by the *kinematic reconstruction equations* (1b). The accuracy of their numerical solution depends directly on the underlying geometry of rigid body motions, which is encoded in the mapping  $\mathbf{A}$ . In the standard MBS formulation the rotations and positions are reconstructed separately according to

$$\begin{pmatrix} \boldsymbol{\omega}_i \\ \mathbf{v}_i^s \end{pmatrix} = \begin{pmatrix} \mathbf{B}_i(\boldsymbol{\theta}_i) & \mathbf{0} \\ \mathbf{0} & \mathbf{I} \end{pmatrix} \begin{pmatrix} \dot{\boldsymbol{\theta}}_i \\ \dot{\mathbf{r}}_i \end{pmatrix}, i = 1, \dots, n. \quad (2)$$

The underlying geometry is that of  $SO(3) \times \mathbb{R}^3$ , which does not account for the coupling of rotations and translation inherent to screw motions. Nevertheless, the kinematic equations (2) correspond to a valid parameterization of rigid body *configurations*. The interdependence of  $\boldsymbol{\omega}_i$  and  $\mathbf{v}_i^s$  is ensured by solving (1a) and (1c), and an analytic solution of (2) correctly reflects the bodies' screw motions. However, when (1) is solved numerically with a finite step size, and (1b) is used to predict finite (screw) *motion* increments, also the kinematic reconstruction equations (1b) must properly reflect the geometry of screw motions. Moreover, (2) can only predict the finite motion if  $\mathbf{r}_i$  are the coordinates of a point on the rotation axis, as for instance in the case of an unconstrained body with its body-fixed reference frame located at the COM. A generic motion of a constrained body, as part of a MBS, will not comply with the decoupling assumption encoded in (2). The matrix  $\mathbf{B}$  is specific to the rotation parameterization. If Euler angles are used, for instance,  $\mathbf{B}$  corresponds to the kinematic Euler equations [45].

Consequently, the kinematic reconstruction equations (1b) shall be amended in order to respect the interrelation of rotations and translations, which boils down to the appropriate choice of the rigid body configuration space being a Lie group. The implications of using the Lie group  $SE(3)$  as well as  $SO(3) \times \mathbb{R}^3$  are studied in this paper.

2. The second issue regards the violations of the constraints (1c) that occur when numerically solving (1). This has been a central problem in numerical MBS dynamics. However, the investigations have exclusively been focussed on reducing or correcting constraint violations by means of stabilization and projection methods [2, 5] rather than aiming to avoid such violations. It is immediately clear that the constraint satisfaction is affected by the accuracy with which the finite motions are reconstructed from the velocity field  $\mathbf{V}$  solving (1a), which indeed depends on the feasibility of the relation (1b). Even more, besides the accuracy with which the system dynamics is captured by the numerical integrator, it is crucial to ensure the kinematic consistency of the MBS, thus the constraint satisfaction is imperative. This is the focus of this paper. In this respect it is important to observe that the majority of mechanisms is built with lower kinematic pairs (Reuleaux pairs). The latter are characterized by their isotropy groups, i.e. subgroups of  $SE(3)$  leaving the contact surface invariant. It is clear that, if a numerical update step does not respect these motion groups, the lower pair constraints will be violated.

The reconstruction equations (1b) represent a first-order relation, and from a computational perspective the question arises whether the decoupling significantly affects the accuracy of the numerical solution of (1). The goal of this paper is to study the extend to which different forms of this first-order relation affect the reconstruction of finite motions of a constrained MBS with numerical time integration methods. To this end, the kinematic reconstruction equations (1b) will be reformulated as an ordinary differential equation (ODE) on the c-space Lie group of the form

$$\widehat{\mathbf{V}}_i = \mathbf{dexp}_{-\boldsymbol{\Phi}_i} \dot{\boldsymbol{\Phi}}_i \quad (3)$$

with  $\boldsymbol{\Phi}_i, \widehat{\mathbf{V}}_i \in \mathfrak{g}$  and  $\mathfrak{g}$  being the Lie algebra of the respective c-space Lie group used to describe the motion of body  $i$ . The two Lie groups considered here are  $SE(3)$  and  $SO(3) \times \mathbb{R}^3$ . In case of  $SE(3)$  the exponential coordinates  $\boldsymbol{\Phi}_i$  are the screw coordinates used to describe the rigid body motions, while in case of  $SO(3) \times \mathbb{R}^3$  they consist of the scaled rotation vector and the Cartesian position coordinates, and (3) reduces to (2). The operator  $\mathbf{dexp}$  is the right-translated differential of the exponential mapping on the c-space Lie group. Hence, the use of a specific c-space is reflected by the corresponding exponential mapping, which clearly leads to different numerical properties of (3).

Spatial kinematics rests on the theory of screws [14, 28]. Instantaneous screw motions form the Lie algebra  $se(3)$  that generates the Lie group  $SE(3)$  of finite rigid body motions. Both are canonically related via the exponential mapping. This fact is the cornerstone of modern kinematics. In context of computational MBS dynamics this fact has not yet been sufficiently exploited, however. Chevalier [23, 24] introduced a coordinate free formulation for the dynamics of tree-topology MBS, which has unfortunately not been recognized by the MBS community. In robotics the Lie group formulation has been given due attention after Brockett [17] introduced the product-of-exponential (POE) formula. This gave rise to Lie group formulations for MBS such

as [46, 47, 48, 60, 58]. Liu in [40] already presented a MBS modeling approach using screw theory and Lie group methods. Now excellent introductions can be found in the text books by Angeles [1], Murray et. al [53], and Selig [62]. On one hand, the Lie group setting provides a framework for systematic matrix formulations of MBS dynamics as discussed in the recent book by Featherstone [32] and Uicker et al. [69] that are tailored for code implementation. On the other hand, it also provides the basis for analytical investigations as reported in [25].

These contributions regard the dynamics modeling of MBS. Even less publications deal with the numerical solution of the MBS motion equations using geometric concepts or Lie group time integration schemes such as the Munthe-Kaas (MK) scheme. The time integration of the rotational dynamics of rigid bodies on the Lie group  $SO(3)$  has been a standard example from the outset of the MK method in [43, 50, 51, 52, 55]. But the MK scheme is only applied to MBS dynamics in few publications such as [59]. In that publication the rigid body motion is considered on  $SE(3)$ , and the dexp mapping in (3) is the one for screw motions.

Recently there is an increased interest in applying Lie group integrators to MBS, mainly motivated by the fact that no global parameterization is needed, thus circumventing the singularity problem of spatial rotations, and that the geometric setting allows preservation of essential invariants. In [19, 21, 39] numerical time stepping schemes were introduced adopting the Newmark/generalized-alpha schemes [30, 54]. A MK integrator is used in [68] to solve the index 1 DAE MBS formulation. All these approaches use  $SO(3) \times \mathbb{R}^3$  as rigid body c-space. The latter does not represent proper rigid body motions. The consequences of this fact for the constraint satisfaction in MBS models have been briefly analyzed in [49]. Along this line numerical results were reported in [20], but without further analysis. As it will be shown in this paper, the crucial point is the preservation of invariants of rigid body motions (only preserved by  $SE(3)$ ). The preservation of invariants is also a central issue in the dynamics of flexible bodies. Geometrically exact formulations rely on the proper representation of large motions, and numerical time stepping schemes should respect the geometric invariants. This has been discussed in [13] where it was shown that a numerical scheme is only invariant w.r.t. to the chosen reference frame if the motion of a frame (rigid body, nodal frame) is represented by  $SE(3)$  (although the Lie group is not mentioned). This is the basis for momentum-preserving integration schemes for finite element models reported in [7, 8, 9, 10], and for an integration scheme in [11] that also respects Newton's third law (actio-reactio principle). Unfortunately the implications of these results for time integration schemes have not been sufficiently recognized. Moreover, occasionally,  $SE(3)$  is wrongly identified with  $SO(3) \times \mathbb{R}^3$  in the literature, e.g. [64].

The aim of this paper is to clarify that any Lie group integrator operating on  $SO(3) \times \mathbb{R}^3$  as rigid body c-space violates the joint constraints in MBS models according to its order of accuracy, whereas using  $SE(3)$  can achieve perfect constraint satisfaction. The latter does not increase the order of accuracy of the applied numerical integration scheme, but it ensures consistency of the MBS model and thus improves the overall accuracy. The problem is addressed for the absolute coordinates (also called inertial coordinates) formulation. where (1a) consists of the Newton-Euler equations of the  $n$  individual bodies and (1c) represents geometric constraints due to lower pair joints. The problem is approached from a kinematic perspective. Numerical aspects of the integration schemes are not a topic of this paper.

The paper is organized as follows. In section 2 the configuration space of a constrained MBS is introduced using  $SE(3)$  and  $SO(3) \times \mathbb{R}^3$  as Lie group, respectively. The MBS motion equations are given in section 3. The classical vector space formulation is presented in terms of independent canonical parameters (screw coordinates). To account for parameterization singularities, a formulation in terms of dual quaternions is also given. Further, a Lie group formulation is reported that is inherently coordinate-free and not prone to singularities. As a numerical integration scheme for this formulation the Munthe-Kaas method is recalled in appendix B. The main result is presented in section 4 where the consequences of using either c-space Lie group for the constraint satisfaction are discussed. It is concluded that  $SE(3)$  yields the best constraint satisfaction at the expense of slightly more complex kinematic relations. Several examples are reported in section 5, and the paper closes with a summary and conclusion in section 6. Regarding the geometric background the reader is referred to the text books [1, 14, 28, 53, 62]. In order to make the paper accessible to reader not familiar with rigid body kinematics and screw theory, the fundamental geometric background is summarized in appendix A. In particular, the semidirect and direct product representation of rigid body motions are discussed. Their parameterization in terms of dual quaternions and ordinary quaternions are recalled. This is important since the parameterization of  $SE(3)$  in terms of canonical (screw) coordinates suffers from the known singularities, and would thus not allow for using the  $SE(3)$  configuration update in the classical vector space MBS formulation.

It is important to emphasize that all considerations in MBS kinematic are related to certain reference frames and that all Lie groups appearing in this context are matrix Lie groups.

## 2 The Configuration Space Lie Group of a Constrained MBS

### 2.1 MBS C-Space in Left-Invariant $SE(3)$ Representation

The Lie group of proper rigid body motions is  $SE(3) = SO(3) \times \mathbb{R}^3$  –the semidirect product of the rotation group and the translation group identified with  $\mathbb{R}^3$  (see appendix A). The *ambient configuration space* of an MBS comprising  $n$  rigid bodies is the  $6n$ -dimensional Lie group (the superscript  $\times$  indicates the semidirect product)

$$G^\times := SE(3)^n. \quad (4)$$

An element  $g = (\mathbf{C}_1, \dots, \mathbf{C}_n) \in G^\times$  represents the configuration of  $n$  decoupled bodies in a coordinate-free way. Multiplication is componentwise and inherited from  $SE(3)$ . The inverse is  $g^{-1} = (\mathbf{C}_1^{-1}, \dots, \mathbf{C}_n^{-1})$ .

The Lie algebra of  $G^\times$  is  $\mathfrak{g}^\times := se(3)^n$  equipped with the Lie bracket inherited componentwise from  $se(3)$  in (49).  $\mathfrak{g}^\times$  is isomorphic to  $(\mathbb{R}^6)^n$  equipped with the componentwise screw product. The notations  $\mathbf{q} = (\mathbf{X}_1, \dots, \mathbf{X}_n) \in (\mathbb{R}^6)^n$  and  $\hat{\mathbf{q}} = (\hat{\mathbf{X}}_1, \dots, \hat{\mathbf{X}}_n) \in \mathfrak{g}^\times$  are used to denote the overall vector of screw coordinates of the MBS. With the exponential mapping on  $SE(3)$  the mapping  $\exp : \mathfrak{g}^\times \rightarrow G^\times$  is

$$\exp \hat{\mathbf{q}} = (\exp \hat{\mathbf{X}}_1, \dots, \exp \hat{\mathbf{X}}_n) \in G^\times. \quad (5)$$

Accordingly its right-translated differential is  $\text{dexp}_{\hat{\mathbf{q}}}(\hat{\mathbf{q}}') = (\text{dexp}_{\hat{\mathbf{X}}_1}(\hat{\mathbf{Y}}_1'), \dots, \text{dexp}_{\hat{\mathbf{X}}_n}(\hat{\mathbf{Y}}_n'))$ . The vector  $\mathbf{q}$  represents the global coordinates of the MBS.

MBS velocities are denoted as  $\mathbf{V} = (\mathbf{V}_1, \dots, \mathbf{V}_n) \in (\mathbb{R}^6)^n$ . The body-fixed MBS twists are introduced as  $\hat{\mathbf{V}} = g^{-1}\dot{g} \in \mathfrak{g}^\times$ . In terms of  $\dot{\mathbf{x}}$  this is  $\hat{\mathbf{V}} = \text{dexp}_{-\hat{\mathbf{q}}}(\dot{\hat{\mathbf{q}}})$ , which can be written in vector form as  $\mathbf{V} = \text{dexp}_{-\mathbf{q}}\dot{\mathbf{q}}$ .

The ambient c-space Lie group allows representing configurations of  $n$  decoupled bodies. It remains to incorporate constraints the MBS is subjected to. It is assumed that the MBS is subjected to a system of  $m$  scleronomic geometric constraints

$$h(g) = \mathbf{0} \quad (6)$$

with the constraint mapping  $h : G^\times \rightarrow \mathbb{R}^m$ . Time differentiation of the geometric constraints gives rise to the velocity constraints

$$\mathbf{J}(g) \cdot \mathbf{V} = \mathbf{0} \quad (7)$$

where  $\mathbf{J}(g) : (\mathbb{R}^6)^n \rightarrow \mathbb{R}^m$  is the Jacobian mapping of  $h$  in vector space representation of  $\mathfrak{g}^\times$ . The geometric constraints define the *MBS configuration space* (an analytic subvariety of the manifold  $G^\times$ )

$$\mathcal{V}^\times := \{g \in G^\times | h(g) = \mathbf{0}\}. \quad (8)$$

(6), (7), and (8) can be expressed in terms of the (local) coordinates  $\mathbf{q} \in \mathfrak{g}^\times$  on  $G^\times$  (screw coordinates). Alternatively, dual quaternions can be used as dependent (global) coordinates, replacing  $SE(3)$  by  $\mathbb{H}_\varepsilon$  (appendix A.4). The couple  $(g, \mathbf{V})$ , or alternatively  $(\mathbf{q}, \mathbf{V})$ , represents the MBS state. The Lie group formulation is merely a formal description of what is commonly pursued in MBS dynamics.

**Remark 1.** *In this paper the 'absolute coordinate' approach for MBS modeling is used. In coordinate-free terms the 'absolute' configuration of each body w.r.t. a global reference frame is represented by  $\mathbf{C}_i$ , and these are subject to certain joint constraints. Rotation and translation parameters can be introduced for each rigid body representing six 'absolute coordinates'.*

### 2.2 MBS C-Space in Left-Invariant $SO(3) \times \mathbb{R}^3$ Representation

The direct product group  $SO(3) \times \mathbb{R}^3$  allows for representing rigid body *configurations* but not rigid body *motions*. The direct product representation corresponds to the mixed velocity representation. The corresponding

ambient configuration space of the MBS is the  $6n$ -dimensional Lie group (the superscript  $\times$  indicates the direct product)

$$G^\times := (SO(3) \times \mathbb{R}^3)^n \quad (9)$$

with elements  $g = (\mathbf{C}, \dots, \mathbf{C}_n) \in G^\times$  and inverse  $g^{-1} = (\mathbf{C}_1^{-1}, \dots, \mathbf{C}_n^{-1})$ . The multiplication is inherited from  $SO(3) \times \mathbb{R}^3$ . The corresponding Lie algebra is  $\mathfrak{g}^\times := (so(3) \oplus \mathbb{R}^3)^n$ , which is isomorphic to  $(\mathbb{R}^6)^n$  equipped with the componentwise Lie bracket (62). Adopting the above notation,  $\mathbf{q} = (\mathbf{X}_1, \dots, \mathbf{X}_n) \in (\mathbb{R}^6)^n$  and  $\hat{\mathbf{q}} = (\hat{\mathbf{X}}_1, \dots, \hat{\mathbf{X}}_n) \in \mathfrak{g}^\times$ , the exponential mapping on  $G^\times$  is introduced as

$$\exp \mathbf{q} = (\exp \mathbf{X}_1, \dots, \exp \mathbf{X}_n) \in G^\times \quad (10)$$

with  $\exp$  in (65), and its differential in an obvious way. The mixed velocity of the MBS is defined with (66) as the left-invariant vector field  $\hat{\mathbf{V}}^m = g^{-1}\dot{g} = (\hat{\mathbf{V}}_1^m, \dots, \hat{\mathbf{V}}_n^m) \in \mathfrak{g}^\times$ . It is determined in vector notation as  $\mathbf{V}^m = \mathbf{dexp}_{-\mathbf{q}}\hat{\mathbf{q}}$  with (68).

Imposing the geometric constraints (6) yields the *MBS configuration space in direct product representation*

$$\mathcal{V}^\times := \{g \in G^\times | h(g) = \mathbf{0}\} \quad (11)$$

The velocity constraints attain the form (7), but now with  $\mathbf{V}^m$ . The  $\mathbf{q} \in \mathfrak{g}^\times$  serve as (local) coordinates on  $G^\times$ . The MBS state is represented by  $(g, \mathbf{V}^m)$  or  $(\mathbf{q}, \mathbf{V}^m)$ . Using quaternions for the rotation part gives rise to an alternative (global) parameterization when  $SO(3) \times \mathbb{R}^3$  is replaced by  $\mathbb{H} \times \mathbb{R}^3$  (appendix A.5).

### 3 Motion Equations of Constrained MBS

#### 3.1 Motion equations on the parameter space in canonical coordinates (axis-angle, position vector)

The constrained motion equations (1) in terms of the non-holonomic quasi-velocities  $\mathbf{V}$  are used as governing equations in descriptor form for the dynamics simulation of constrained MBS in terms of absolute coordinates  $\mathbf{q}$ . To account for a general c-space Lie group, the kinematic reconstruction equations (1b) are expressed in terms of the  $\mathbf{dexp}$  mapping, which gives rise to the formulation

$$\mathbf{M}(\mathbf{q})\dot{\mathbf{V}} + \mathbf{J}^T \boldsymbol{\lambda} = \mathbf{Q}(\mathbf{q}, \mathbf{V}, t) \quad a) \quad (12)$$

$$\mathbf{V} = \mathbf{dexp}_{-\mathbf{q}}\hat{\mathbf{q}} \quad b) \quad (12)$$

$$h(\mathbf{q}) = \mathbf{0}. \quad c) \quad (12)$$

The choice of 'absolute coordinates' depends on the c-space Lie group. Using  $G^\times$  as c-space,  $\mathbf{q} \in \mathfrak{g}^\times$  comprises the  $n$  screw coordinate vectors  $\mathbf{X}_i = (\boldsymbol{\xi}_i, \boldsymbol{\eta}_i)$ , and when using  $G^\times$ ,  $\mathbf{q} \in \mathfrak{g}^\times$  comprises the  $n$  vectors  $\mathbf{X}_i = (\boldsymbol{\xi}_i, \mathbf{r}_i)$ . In either case,  $\mathbf{q}$  are local coordinates and  $\mathfrak{g} \simeq \mathbb{R}^{6n}$  is the parameter space. Accordingly,  $\mathbf{V}$  consists of body-fixed twists or mixed velocities. With the 'absolute coordinate approach' the system (12a) summarizes the Newton-Euler equations governing the dynamics of the  $n$  bodies subject to the geometric constraints (12c). This an index 3 DAE system. The dynamics of the MBS is represented as the dynamics of the representing point  $\mathbf{q}$  on the subvariety  $h^{-1}(\mathbf{0}) \subset G$ . It is commonly treated as an ODE on a vector space by considering the parameter space as vector space. To this end (12a) and the acceleration constraints  $\mathbf{J}(\mathbf{q}) \cdot \dot{\mathbf{V}} = \boldsymbol{\eta}(\mathbf{q}, \mathbf{V})$  (second time derivative of (12c)) are combined to the index 1 system

$$\begin{pmatrix} \mathbf{M} & \mathbf{J}^T \\ \mathbf{J} & \mathbf{0} \end{pmatrix} \begin{pmatrix} \dot{\mathbf{V}} \\ \boldsymbol{\lambda} \end{pmatrix} = \begin{pmatrix} \mathbf{Q} \\ \boldsymbol{\eta} \end{pmatrix}. \quad (13)$$

For a given state  $(\mathbf{q}, \mathbf{V})$  of the MBS, (13) can be solved for  $\dot{\mathbf{V}}$  and  $\boldsymbol{\lambda}$  giving rise to an explicit ODE  $\dot{\mathbf{V}} = F(\mathbf{q}, \mathbf{V})$  and thus replacing (12) by

$$\dot{\mathbf{V}} = F(\mathbf{q}, \mathbf{V}) \quad a) \quad (14)$$

$$\hat{\mathbf{q}} = \mathbf{dexp}_{-\mathbf{q}}^{-1} \mathbf{V} \quad b). \quad (14)$$

This general formulation of MBS motion equations is applicable to any c-space Lie group. The velocities  $\mathbf{V}$  are either body-fixed twists or mixed velocities. A specific choice for the rigid body c-space, with corresponding dexp mapping, leads to a specific ODE system (14b). If  $G^\times$  and a 3-parametric description of rotations are used, (14b) attains the particular form (2) with (59), which is commonly applied in MBS formulations. In any case the motion equations are treated as a system on  $\mathbb{V}^n$  considered as vector space.

**Remark 2.** *Analytically any kinematic relation in (12b) is admissible that corresponds to a valid parameterization of rigid body configurations (not necessarily motions). Even if the coupling of angular and linear velocities are not respected by (12b) and (14b), as with (68), any kinematic reconstruction equation will yield the same analytic solution since this dependence is respected by the solution of (12a). But this is not true when numerically solving (12) as shown in the remainder of this paper since then (12b) is used to estimate finite motions.*

**Assumption:** It is assumed in the following that the velocity constraints are satisfied.

This assumption is made in order to focus on the configuration update. The consistency of the velocity with the linear velocity constraints can be easily achieved by a one-step projection if necessary. In all examples below, and for the majority of complex MBS, the numerical solution for  $\mathbf{V}$  at time step  $i$  satisfies the velocity constraints when starting with one at time step  $i - 1$  that satisfies them.

### 3.2 Motion equations in dependent coordinates (quaternions)

Any parameterization of rigid bodies in terms of six independent parameters leads to parameterization singularities, caused by 3-parameter description of rotations. To circumvent this problem, dual quaternions and Euler parameters can be used giving rise to a singularity-free parameterization of  $SE(3)$  and  $SO(3) \times \mathbb{R}^3$ , respectively (appendix A.3 and A.4). In terms of these parameters, summarized in the generalized coordinate vector  $\mathbf{q}$ , the motion equations are

$$\dot{\mathbf{V}} = F(\mathbf{q}, \mathbf{V}) \quad a) \quad (15)$$

$$\dot{\mathbf{q}} = \mathbf{H}^{-1}(\mathbf{q})\mathbf{V} \quad b) \quad (15)$$

where the coefficient matrix in (15b) is either (78) for  $SE(3)$ , or (80) for  $SO(3) \times \mathbb{R}^3$ , or (76) if mixed velocities are used in the  $SE(3)$  formulation. The use of dependent parameters introduces further constraints due to the normalization and Plücker condition. These constraints are included in (12c), and are accounted for by the constraint Jacobian. The motion equations are again treated as system on a vector space.

It is straightforward to evaluate  $F$  in (15a) when the rotation matrices of the bodies are replaced by  $\mathbf{R} = \mathbf{D}\mathbf{E}^T$  in (73) and the position vectors by  $\mathbf{r}$  in (74). It is just remarked here that the motion equations can also be consistently formulated in terms of dual quaternions [18, 29].

### 3.3 Motion equations on the c-space Lie group

The best way to avoid parameterization singularities is to not use local parameters at all. Instead of introducing local coordinates  $\mathbf{q}$ , rigid body configurations are represented coordinate-free by  $g \in G^\times$  or  $g \in G^\times$ . The velocities  $\mathbf{V}$  belong to the respective Lie algebra. Then the constrained motion equations attain the form

$$\mathbf{M}(g)\dot{\mathbf{V}} + \mathbf{J}^T\boldsymbol{\lambda} = \mathbf{Q}(g, \mathbf{V}, t) \quad a) \quad (16)$$

$$\dot{g} = g\widehat{\mathbf{V}} \quad b) \quad (16)$$

$$h(g) = \mathbf{0}. \quad c) \quad (16)$$

where, instead of using a parameterization, the reconstruction equations (16b) are merely the (coordinate-free) definition of twists, either (48) or (66). With a solution  $\dot{\mathbf{V}} = F(g, \mathbf{V})$  of (13) this leads to the motion equations

$$\dot{\mathbf{V}} = F(g, \mathbf{V}) \quad a) \quad (17)$$

$$\dot{g} = g\widehat{\mathbf{V}}. \quad b) \quad (17)$$

Overall (17) is an ODE system on the MBS state space  $\mathfrak{g} \times G$ . The system (17b) is an ODE on the c-space Lie group  $G$ , and equations (17a) form an ODE on the vector space  $\mathfrak{g} \cong \mathbb{R}^{6n}$ , as in (14). The latter can be solved with any established numerical (vector space) integration scheme, whereas solution of (17b) requires

application of a Lie group integration scheme, where local parameters will have to be used eventually. In this way the parameterization problem is shifted to the integration scheme [19, 21, 31, 39, 68]. A widely used integration scheme for ODE on Lie groups is the explicit MK method, which is briefly recalled in appendix B. These schemes implicitly define a local parameter chart around the current configuration.

#### 4 The significance of the configuration space for numerical reconstruction of rigid body motions constrained to subgroups

The fact that most joints in MBS models constrain the relative motion of adjacent bodies to  $SE(3)$  subgroups (in particular Reuleaux lower pairs) seems to put the use of the direct product group into perspective. Since in the absolute coordinate formulation the update step adjusts the absolute configuration bodies, the semidirect representation does not necessarily preserve the lower pair constraints, however.

Given the velocity of a body, its finite motion is the solution of the kinematic reconstruction equations (53) (respectively (68)). Since either formulation is consistent with the respective definition of velocity, both yield the same *analytical* solution for the MBS motion (but in terms of different coordinates). The difference of the formulations is critical, however, when the reconstruction equations are solved numerically and used to estimate finite motions.

When numerically solving (14b) with a (explicit or implicit) numerical vector space integration scheme, a constant screw coordinate vector  $\Phi^{(i)} \in \mathfrak{g}$  is constructed and used to estimate the finite configuration at integration step  $i$  as  $g(t_i) = \exp \hat{\mathbf{q}}^{(i)}$  with  $\mathbf{q}^{(i)} = \mathbf{q}^{(i-1)} + \Phi^{(i)}$ . When integrating (17b) with a Lie group integrator such as a Munthe-Kaas (MK) integration scheme (83), a  $\Phi^{(i)}$  is constructed that determines the configuration increment  $\exp \hat{\Phi}^{(i)}$ . Hence, regardless of the particular integration scheme, a finite estimate is found by evaluating the dexp mapping. The latter locally reflects the geometry of the configuration space, and clearly using either  $SO(3) \times \mathbb{R}^3$  or  $SE(3)$ , the respective dexp mapping yields different changes of the local coordinates  $\Phi$  for the same twist, which is uniquely determined by the dynamic equations (14a). Nevertheless the finite motion estimates are in accordance with the respective geometric model, but not necessarily with the MBS kinematics. Thus the difference boils down to the geometry of the c-space. Consequently, only the  $SE(3)$  update can possibly lead to proper estimates of constrained rigid body motions.

A numerical integration scheme estimates  $\Phi^{(i)}$  as a (usually) linear combination of  $\mathbf{dexp}^{-1}$  in (14b) when evaluated at intermediate time steps  $j = 1, \dots, s$  of the (possibly implicit) numerical integrator. Using (43), which applies to any Lie group, a general integration step can be written as

$$\Phi^{(i)} = \sum_{j=1}^s \sum_{r=0}^{\infty} \alpha_{ij} \mathbf{ad}_{\mathbf{V}^{(j)}}^r \mathbf{V}^{(i)} \quad (18)$$

denoting  $\mathbf{V}^{(j)} := \mathbf{V}(t_{i-1} + c_j \Delta t, \mathbf{q}_j)$  with some real coefficients  $\alpha_{rj}$  and  $c_j$  specific to the integration scheme. That is,  $\Phi^{(i)}$  is given in terms of nested Lie brackets of body velocities at intermediate time steps  $t_{i-1} + c_j \Delta t$ . Hence, the so determined  $\Phi^{(i)}$  belongs to the smallest Lie subalgebra of  $\mathfrak{g}$  containing the absolute body twists  $\mathbf{V}$ . This is a screw algebra [34, 35, 37, 62] if  $SE(3)$  is used as c-space. The configuration increment  $g(t_i)$  belongs to the corresponding subgroup of the c-space Lie group  $G$ , sometimes called the *completion group*.

For the finite update step to respect the geometric constraints it is thus necessary that the constrained absolute motion belongs to a subgroup of the c-space Lie group. Since a configuration update step yields  $\Phi^{(i)}$  in the subalgebra generated by the twists, this condition is also sufficient.

**Corollary 1.** *The kinematic motion constraints of a body in a MBS are satisfied by a configuration update step in terms of linear combinations of velocity samples  $\mathbf{V}^{(j)}$  if its motion is constrained to a subgroup of its c-space Lie group.*

This corollary applies to a general c-space Lie group. Understanding the implications for a specific choice requires inspection of the possible subgroups.

The direct product group  $SO(3) \times \mathbb{R}^3$  possesses the following subgroups: The groups with elements  $C = (\mathbf{I}, \mathbf{r})$ , representing pure 1, 2, or 3 dimensional translations; the groups with elements  $C = (\mathbf{R}, \mathbf{0})$ , representing pure 1 or 3 dimensional rotations such that the origin of body-fixed and spatial frame coincide; and the groups with elements  $C = (\mathbf{R}, \mathbf{r})$ , representing decoupled 1 or 3 dimensional rotation and 1, 2, or 3 dimensional translation. It is crucial to notice that the elements  $C = (\mathbf{R}, \mathbf{0})$  cannot represent rotations about arbitrary axes/points since this would lead to non-zero  $\mathbf{r}$ . Clearly these groups have limited practical relevance.

The 11 subgroups of  $SE(3)$ , on the other hand, do have a practical significance including modeling of lower pair joints that correspond to six of the  $SE(3)$  subgroups [62] and are used in MBS modeling. Moreover,

also the other  $SE(3)$  subgroups are used in MBS modeling (occasionally referred to as 'macro-joints'). The immediate consequence is that the constraints imposed by a lower pair joint connecting a rigid body to the ground are exactly satisfied by an  $SE(3)$  update step.

To illustrate the effect of the two formulations of update steps, consider the kinematic reconstruction equations  $\dot{\mathbf{X}} = \mathbf{dexp}_{-\mathbf{X}}^{-1} \mathbf{V}$  in the time interval  $[t_i, t_{i+1}]$ , with  $\mathbf{X}(t_i) = \mathbf{0}$  applied to a body rotating with constant angular velocity  $\omega_0$  about a constant rotation axis  $\boldsymbol{\xi}$  at a position  $\mathbf{p}$  in figure 1a). The reference frame performs a coupled rotation and translation. Using  $SE(3)$  as c-space, the motion belongs to its subgroup  $SO(2)$ . If  $SO(3) \times \mathbb{R}^3$  is used as c-space, the motion only forms a submanifold.

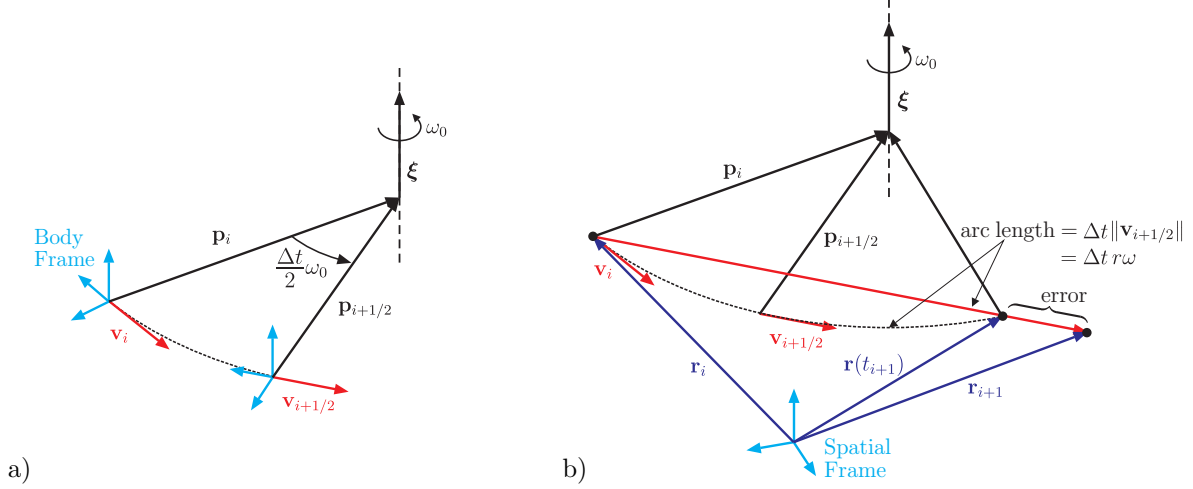


Figure 1. a) Frame rotating about a fixed axis with constant angular velocity. b) Position error when using the  $SO(3) \times \mathbb{R}^3$  update.

The body-fixed twist of the reference frame is  $\mathbf{V} = (\omega \boldsymbol{\xi}, \omega \mathbf{p} \times \boldsymbol{\xi})$ . For illustration purpose, the simple explicit trapezoidal integration scheme is applied. In standard vector space form, applied to solve  $\dot{x} = f(t, x)$ , the latter reads

$$k_1 = f(t_i, x_i), \quad k_2 = f\left(t_i + \frac{\Delta t}{2}, x_i + \frac{\Delta t}{2} k_1\right)$$

$$x_{i+1} = x_i + \Delta t k_2$$

where  $\Delta t$  is the time step size. Applied to the kinematic equations on the c-space Lie group, this is

$$\mathbf{k}_1 = \mathbf{dexp}_{-\boldsymbol{\xi}_i}^{-1} \mathbf{V}_i = \mathbf{V}_i, \quad \mathbf{k}_2 = \mathbf{dexp}_{-\frac{\Delta t}{2} \mathbf{k}_1}^{-1} \mathbf{V}_{i+1/2} = \mathbf{dexp}_{-\frac{\Delta t}{2} \mathbf{V}_i}^{-1} \mathbf{V}_{i+1/2}$$

$$\boldsymbol{\xi}_{i+1} = \boldsymbol{\xi}_i + \Delta t \mathbf{k}_2 = \Delta t \mathbf{dexp}_{-\frac{\Delta t}{2} \mathbf{V}_i}^{-1} \mathbf{V}_{i+1/2} \approx \Delta t \mathbf{V}_{i+1/2} - \frac{\Delta t^2}{4} [\mathbf{V}_i, \mathbf{V}_{i+1/2}] + \dots$$

$$\mathbf{C}_{i+1} = \mathbf{C}_i \exp \boldsymbol{\xi}_{i+1}$$

with  $\mathbf{V}_i = \mathbf{V}(t_i)$ ,  $\mathbf{V}_{i+1/2} = \mathbf{V}(t_i + \Delta t/2)$ , and noting that  $\boldsymbol{\xi}_i = \mathbf{0}$ . Denote with  $\mathbf{p}_i$  and  $\mathbf{v}_i = \omega \mathbf{p}_i \times \boldsymbol{\xi}_i$  the position and linear velocity vector, respectively, at time  $t_i$  (figure 1a). Since  $\omega_0$  is constant,  $\mathbf{p}_i = \mathbf{p}$  and  $\mathbf{v}_i = \mathbf{v}$  expressed in the body-fixed frame, and thus  $\mathbf{V}_i$  are constant. Hence the trapezoidal rule yields

$$\boldsymbol{\xi}_{i+1} = \Delta t \mathbf{V}_{i+1/2} = \Delta t \mathbf{V}_i = \Delta t (\omega_0 \boldsymbol{\xi}, \omega_0 \mathbf{p} \times \boldsymbol{\xi})$$

$$\mathbf{C}_{i+1} = \mathbf{C}_i \exp (\Delta t (\omega_0 \boldsymbol{\xi}, \omega_0 \mathbf{p} \times \boldsymbol{\xi})). \quad (19)$$

Apparently,  $(\boldsymbol{\xi}, \mathbf{p} \times \boldsymbol{\xi})$  are the Plücker coordinates of the screw motion of the body, when rotating about the axis  $\boldsymbol{\xi}$  at a distance  $\mathbf{r}$ , so that (19) is in fact the exact solution.

In contrast, if the mixed velocity (66) and the dexp mapping (67) on  $SO(3) \times \mathbb{R}^3$  is used, then the orientation update is exact but the position (vector space) update  $\mathbf{r}_{i+1} = \mathbf{r}_i + \Delta t \mathbf{v}_{i+1/2}$  is not correct as apparent from



figure 1b). This is due to the independent treatment of orientations and translations. Hence  $SE(3)$  is the proper c-space for this example.

This example confirms corollary 1. The perfect constraint satisfaction is possible (for any integration scheme) because the body is connected to the ground by a lower pair joint. Moreover, the corollary regards the motion of constrained bodies rather than their relative motions, i.e. the joint motions. Since the joint constraints are the actual constraints included in the motion equations (1), a statement regarding the joint constraints is in order.

**Lemma 2.** *Consider two bodies constrained to a c-space subgroup  $G_1$  and  $G_2$ , respectively. If their relative motions form a subgroup  $H$ , i.e.  $G_2 = G_1 \cdot H$ , then the relative motion constraints as well as the constraints on the motion of the two bodies are satisfied by any numerical configuration update step in terms of linear combinations of velocity samples.*

**Proof.** The proof follows immediately from the assumption that the group  $G_2$  is the product of the groups  $G_1$  and  $H$ , and thus  $H = G_2/G_1$ . That is,  $g_1g_2 \in H$  for any  $g_1 \in G_1, g_2 \in G_2$ . Hence, since any update of the bodies' motion belongs to the respective subgroup  $G_1$  and  $G_2$ , the relative motion will be in  $H$ . ■

The situation of this lemma is a rather special case since the product of two groups is not necessarily a group itself. A special case is the rigid body connected to the ground by a lower pair joint. In this case, the corollary 1 and lemma 2 are automatically satisfied with  $G_1 = \{I\}$  and  $G_2 = H \subset SE(3)$ , if  $SE(3)$  is used as c-space. This is not so if  $SO(3) \times \mathbb{R}^3$  is used.

As outlined above, lower kinematic pairs form  $SE(3)$  subgroups, while  $SO(3) \times \mathbb{R}^3$  subgroups have almost no practical relevance. The only practically relevant exception where the rigid body motions form a subgroup of  $SO(3) \times \mathbb{R}^3$  is the case of an unconstrained free body with its reference frame attached to the center of mass (COM) (section 5.1).

When lemma 2 does not hold, the joint constraints will not be satisfied exactly. In this case, since both formulations use a first-order relation consistent with the respective kinematic model to estimate the update, the order of accuracy obtained with the  $SE(3)$  and with the  $SO(3) \times \mathbb{R}^3$  update is the same, and the constraint violations are determined by the accuracy of the integration scheme.

**Corollary 3.** *For general MBS, the  $SE(3)$  and the  $SO(3) \times \mathbb{R}^3$  update achieve the same order of accuracy. The  $SE(3)$  update achieves exact satisfaction of geometric constraints for those joints for which lemma 2 holds.*

**Remark 3.** *When the condition of corollary 1 holds, the motion constraints of bodies are perfectly satisfied. The joint constraints are satisfied if lemma 2 holds. It must be emphasized that this does not imply any increase of the order of accuracy of the overall numerical solution. But satisfaction of geometric constraints is vital for the numerical integration. Even more, numerical integration of constrained MBS (using the index 1 formulation (13)) consists of two parts: 1) the numerical integration of the ODE (14) and 2) the stabilization of constraints. The latter is computationally expensive and any means to avoid constraint violations is beneficial. Note that the conclusion applies to the 'standard' vector space formulation (14) in 'local' coordinates as well as to the Lie group integration scheme for the formulation (16).*

## 5 Examples

All examples consist of rigid bodies either unconstrained or subjected to geometric constraints imposed by lower pair joints, and the dynamics equations (12a), respectively (16a), are the Newton-Euler equations. The explicit form of the latter depends on the velocity representation (body-fixed twists, mixed velocities), thus the c-space Lie group, and the used reference frame.

Results are reported when the Lie group formulation (17) is numerically integrated using time step sizes  $\Delta t = 10^{-2}\text{s}, 10^{-3}\text{s}, 10^{-4}\text{s}$ . The dynamic equations (17) are integrated with the Runge-Kutta 4 (RK4) scheme, and the kinematic equations are solved with the MK method (83) based on the RK4 scheme, using the  $SE(3)$  and  $SO(3) \times \mathbb{R}^3$  update, respectively.

It should be recalled that the primary interest here is the accuracy of constraint satisfaction rather than that of the solution  $\mathbf{q}(t)$ . The latter depends indeed on the numerical integration scheme.

### 5.1 Unconstrained Rigid Body – Reference Frame at COM

An unconstrained rigid body is considered assuming that there are no applied or gravitational forces. Although no kinematic constraints are present, the momentum conservation imposes motion invariants. The body-fixed reference frame is located at its COM. The configuration of the body, i.e. of the reference frame, is represented

by  $C = (\mathbf{R}, \mathbf{r}^s)$  with  $\mathbf{r}^s$  being the position vector of the COM expressed in the space-fixed inertial frame and  $\mathbf{R}$  the rotation matrix transforming coordinates from body-fixed reference frame to inertia frame.

In this example the rigid body is a homogenous box with side lengths  $0.8 \times 0.4 \times 0.1$  m made of aluminium. Its mass is  $m = 86.4$  kg and its inertia tensor w.r.t. the COM is  $\Theta_0 = \text{diag}(1.224, 4.68, 5.76)$  kg m<sup>2</sup>.

**5.1.1 Body-Fixed Newton-Euler Equations on  $SE(3)$ .** The dynamics of the body is governed by the Newton-Euler equations. Considering  $C \in SE(3)$ , the body velocity represented in the body-fixed COM frame is a proper twist  $\mathbf{V} = (\boldsymbol{\omega}, \mathbf{v}) \in se(3)$ , and the Newton-Euler equations attain the consistent form

$$\mathbf{J}_0 \dot{\mathbf{V}} - \text{ad}_{\mathbf{V}}^* \mathbf{J}_0 \mathbf{V} = \mathbf{W} \quad (20)$$

where  $\mathbf{W} = (\mathbf{M}, \mathbf{F}) \in se^*(3)$  is the applied wrench expressed in the COM frame, and

$$\mathbf{J}_0 = \begin{pmatrix} \Theta_0 & \mathbf{0} \\ \mathbf{0} & m\mathbf{I} \end{pmatrix} \quad (21)$$

is the inertia matrix w.r.t. to the COM frame. The matrix  $\text{ad}_{\mathbf{V}}^* = \text{ad}_{\mathbf{V}}^T$  is given by (50). The system (20) are the Euler-Poincare equations on  $SE(3)$ .

**5.1.2 Newton-Euler Equations on  $SO(3) \times \mathbb{R}^3$ .** In the mixed velocity representation, the angular velocity  $\boldsymbol{\omega}$  is expressed in the body-fixed COM frame whereas the linear velocity of the COM is expressed in the space-fixed inertial frame, denoted  $\mathbf{v}^s = \dot{\mathbf{r}}$ . The corresponding Newton-Euler equations, written w.r.t. the COM frame, are

$$\begin{pmatrix} \Theta_O & \mathbf{0} \\ \mathbf{0} & m\mathbf{I} \end{pmatrix} \begin{pmatrix} \dot{\boldsymbol{\omega}} \\ \dot{\mathbf{v}}^s \end{pmatrix} + \begin{pmatrix} \hat{\boldsymbol{\omega}} \Theta_O \boldsymbol{\omega} \\ \mathbf{0} \end{pmatrix} = \begin{pmatrix} \mathbf{M} \\ \mathbf{F}^s \end{pmatrix} \quad (22)$$

where  $\mathbf{F}^s$  is the applied force expressed in the inertial frame. The equations (22) can be expressed as the are the Euler-Poincare equations on  $SO(3) \times \mathbb{R}^3$ :  $\mathbf{J}_0 \dot{\mathbf{V}} - \text{ad}_{\mathbf{V}}^* \mathbf{J}_0 \mathbf{V} = \mathbf{W}$  with  $\mathbf{W}^m = (\mathbf{M}, \mathbf{F}^s)$  and (63).

**5.1.3 Numerical Results.** The two formulations are integrated with the MK method using the time step sizes  $\Delta t = 10^{-2}$ s,  $10^{-3}$ s,  $10^{-4}$ s. The initial configuration of the body is set to  $C_0 = (\mathbf{I}, \mathbf{0})$ .

**Spatial Rotation** Setting the initial angular velocity to  $\boldsymbol{\omega}_0 = (10\pi, 2\pi, 0)$  rad/s and  $\mathbf{v}_0 = \mathbf{0}$ , the unconstrained unforced body should rotate about its COM. That is, the vector  $\mathbf{r}^s$  should remain zero. The motion equations are integrated for 10 s.

Both formulations exactly preserve the COM position  $\mathbf{r}^s = \mathbf{0}$ . It is clear that both formulations perform identical since for a pure rotation about the COM the  $SE(3)$  reduces to the  $SO(3) \times \mathbb{R}^3$  formulation. This is visible from the drift of the kinetic energy, shown in figure 2, which should be preserved.

**Rotation about fixed axis plus linear translation** The initial velocities are set to  $\boldsymbol{\omega}_0 = (0, 0, 2\pi)$  rad/s and  $\mathbf{v}_0 = (10, 0, 0)$  m/s. Since the body is unconstrained and no gravity forces are present, it should perform a translation of its COM along the global  $x$ -axis together with a rotation about the global  $z$ -axis. The analytic solution for the position vector is  $\mathbf{r}^s(t) = (t, 0, 0)$  m/s and for the rotation angle  $\varphi(t) = 2\pi t$ . Figure 3 show the position errors for the numerical solutions. For the translation the  $SO(3) \times \mathbb{R}^3$  update yields very good reconstruction for any step size while the accuracy achieved with the  $SE(3)$  update depends on the step size. Clearly visible is the 4th order convergence of the MK method. The rotation update performs equally for both variants, as shown in figure 4, where the relative rotation angle  $\varepsilon_r := \|\log(\mathbf{R}(t)^T \mathbf{R}_{\text{num}})\|$  of the analytic solution  $\mathbf{R}(t)$  and the respective numerical solution  $\mathbf{R}_{\text{num}}$  are shown. Notice that the accuracy is within the computation precision. The figures show essentially the error amplified by the log mapping.

Due to the momentum conservation, the body performs translation along  $x$ -axis plus rotation about  $z$ -axis. This is kinematically equivalent to a rolling disk of radius  $r = \|\mathbf{v}_0\| / \|\boldsymbol{\omega}_0\|$ . This means that the body can be considered being subjected to a kinematic rolling constraint, or in other words being connected to the ground by a higher kinematic pair whose motions do not form a  $SE(3)$  subgroup. It is a subgroup of  $SO(3) \times \mathbb{R}^3$ , however. In fact, the decoupled rotation and translation is the ideal situation for the  $SO(3) \times \mathbb{R}^3$  update, and according to the corollary 1 it should satisfy the motion constraints.

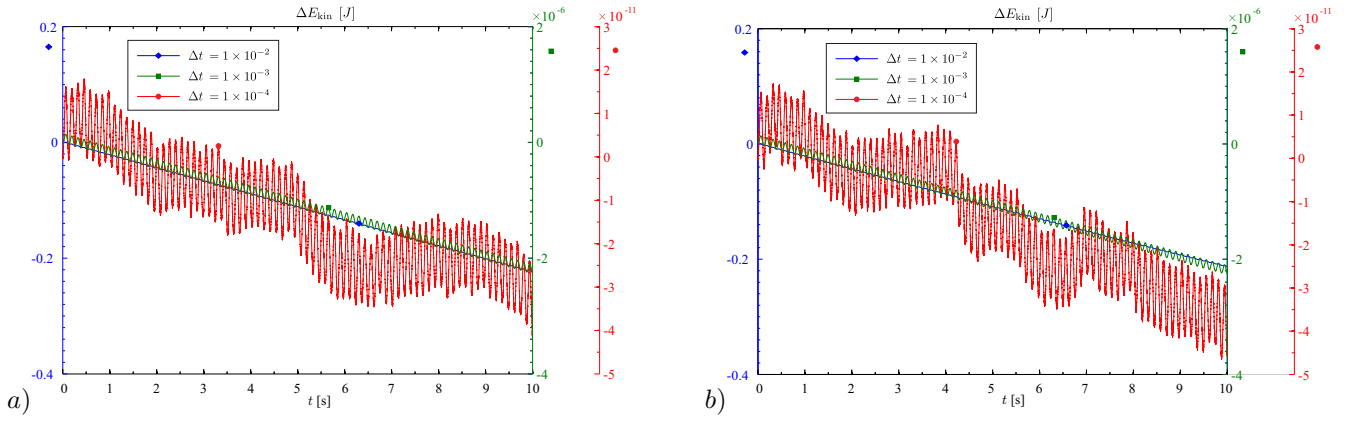


Figure 2. Drift of kinetic energy when integrating a) the  $SE(3)$ , and b) the  $SO(3) \times \mathbb{R}^3$  formulation.

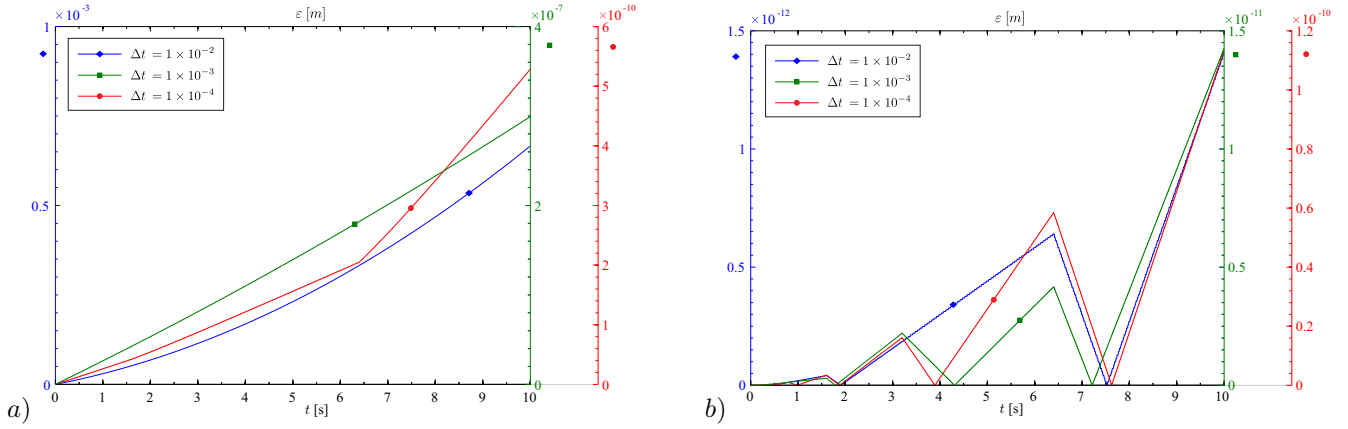


Figure 3. Drift of COM from analytic solution when integrating a) the  $SE(3)$ , and b) the  $SO(3) \times \mathbb{R}^3$  formulation.

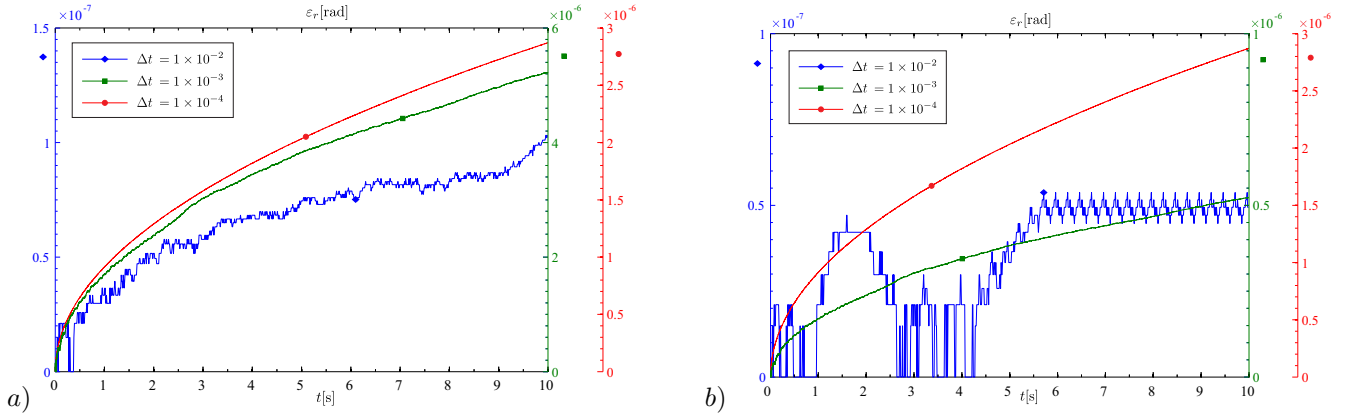


Figure 4. Drift  $\varepsilon_r$  of the orientation from analytic solution when integrating a) the  $SE(3)$ , and b) the  $SO(3) \times \mathbb{R}^3$  formulation.

## 5.2 Unconstrained Rigid Body – Arbitrary Body-Fixed Reference Frame

Besides geometric constraints, another cause of coupling of rotations and translations is the use of body-fixed reference frames not located at the COM. Consider again the rigid body from the previous example, but now with a reference frame parallel translated to an arbitrary body-fixed point  $P$ , i.e. now  $C = (\mathbf{R}, \mathbf{r}^s)$  represents the configuration of this reference frame. Denote with  $\mathbf{r}_0 = (0.4, 0, 0)$  m the COM location expressed in the body-fixed reference frame. Then, transforming the inertia tensor  $\Theta_0$  to the reference frame yields the inertia tensor  $\Theta_P = \text{diag}(1.224, 18.504, 19.584)$  kg m<sup>2</sup>. The motion of the body is indeed the same regardless of the used reference frame, but the motion of the introduced reference frame varies with its location. This has implications for the numerical configuration update.

**5.2.1 Body-Fixed Newton-Euler Equations on  $SE(3)$ .** The Newton-Euler equations (20) are coordinate invariant, and using body-fixed velocities the dynamics of the body is still governed by (20), but now with

$$\mathbf{J}_P = \begin{pmatrix} \boldsymbol{\Theta}_P & -m\hat{\mathbf{r}}_0^T \\ -m\mathbf{R}\hat{\mathbf{r}}_0 & m\mathbf{I} \end{pmatrix} \quad (23)$$

where  $\mathbf{M}, \mathbf{F}$  are expressed in the reference frame. The vector  $\mathbf{V} = (\boldsymbol{\omega}, \mathbf{v})$  is the twist of the reference frame at  $P$ .

**5.2.2 Newton-Euler Equations on  $SO(3) \times \mathbb{R}^3$ .** The Newton-Euler equations are no longer decoupled if the reference frame is not at the COM, and (22) must be replaced by

$$\begin{pmatrix} \boldsymbol{\Theta}_P & -m(\mathbf{R}\hat{\mathbf{r}}_0)^T \\ -m\mathbf{R}\hat{\mathbf{r}}_0 & m\mathbf{I} \end{pmatrix} \begin{pmatrix} \dot{\boldsymbol{\omega}} \\ \dot{\mathbf{v}}^s \end{pmatrix} + \begin{pmatrix} \hat{\boldsymbol{\omega}}\boldsymbol{\Theta}_P\boldsymbol{\omega} \\ \mathbf{R}\hat{\boldsymbol{\omega}}\hat{\boldsymbol{\omega}}\mathbf{r}_0 \end{pmatrix} = \begin{pmatrix} \mathbf{M} \\ \mathbf{F}^s \end{pmatrix}. \quad (24)$$

$\mathbf{V}^m = (\boldsymbol{\omega}, \mathbf{v}^s)$  is the mixed velocity of the reference frame at  $P$ .

**5.2.3 Numerical Results.** As above the initial configuration of the body is set to  $C_0 = (\mathbf{I}, \mathbf{0})$ , and the dynamic equations are integrated with three different time step sizes.

**Spatial Rotation** The situation is the same as in the previous section, where the initial angular velocity is  $\boldsymbol{\omega}_0 = (10\pi, 2\pi, 0)$  rad/s and the COM is at rest. When the body is rotating about its COM the reference frame exhibits the initial linear velocity  $\mathbf{v}_0 = \mathbf{r}_0 \times \boldsymbol{\omega}_0$ . Again, the unconstrained body without gravity forces should perform rotations about its COM. That is, the vector  $\Delta\mathbf{r} = \mathbf{r} - \mathbf{r}_0$  should remain zero. Figure 5 shows the drift  $\varepsilon := \|\Delta\mathbf{r}\|$  of the COM position. The position accuracy achieved by the  $SE(3)$  update is within the computation accuracy of  $10^{-15}$  for all step sizes, while that achieved with the  $SO(3) \times \mathbb{R}^3$  formulation depends on the integration step size. Both formulations achieve the same rotation update and exhibit identical drift of the kinetic energy  $T_0 = 696.399$  J (not shown here). Note that the  $SE(3)$  update satisfies the constraints for arbitrary time step sizes.

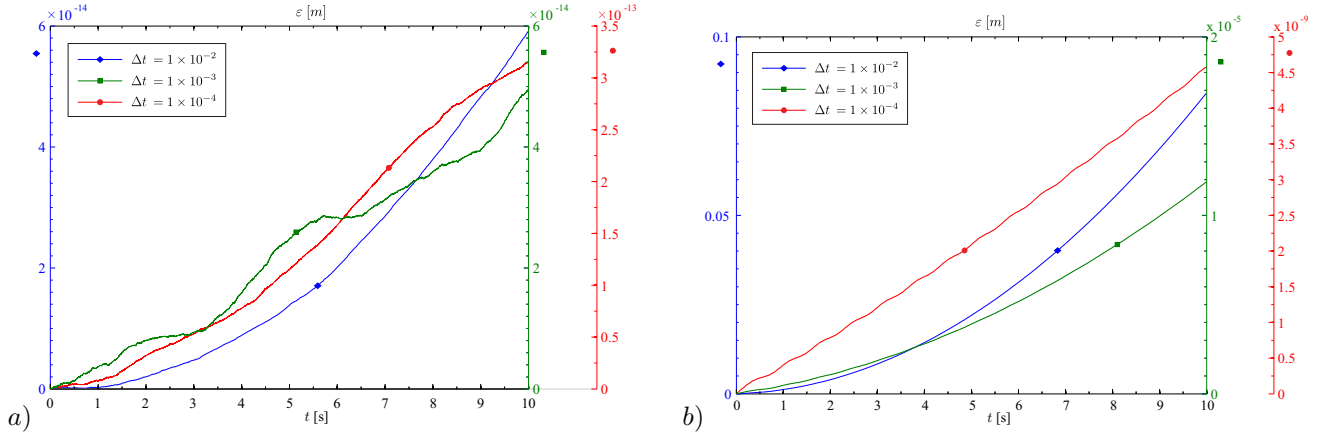


Figure 5. Drift  $\varepsilon$  of the COM when integrating a) the  $SE(3)$ , and b) the  $SO(3) \times \mathbb{R}^3$  formulation.

**Rotation about fixed axis plus linear translation** If, in addition to the initial angular velocity  $\boldsymbol{\omega}_0 = (10\pi, 2\pi, 0)$  rad/s, the body is again given a constant initial linear velocity of 10 m/s, the initial velocity of the reference frame is  $\mathbf{v}_0 = \mathbf{r}_0 \times \boldsymbol{\omega}_0 + (10, 0, 0)$  m/s. The body performs the same spatial rotation as above together with the linear motion of its COM, i.e. a screw motion of the reference frame.

Figure 6 reveals that the accuracy of both formulations depends on the step size. The  $SO(3) \times \mathbb{R}^3$  update yields the best accuracy as for the above model with the reference frame at the COM. As for the above model, the

lower accuracy of the  $SE(3)$  update is attributed to the fact that the motion does not belong to a subgroup. The result is to be expected since the  $SE(3)$  update scheme is frame invariant. Also the  $SO(3) \times \mathbb{R}^3$  update cannot exactly estimate the finite motion since with the chosen reference frame this does not belong to a subgroup.

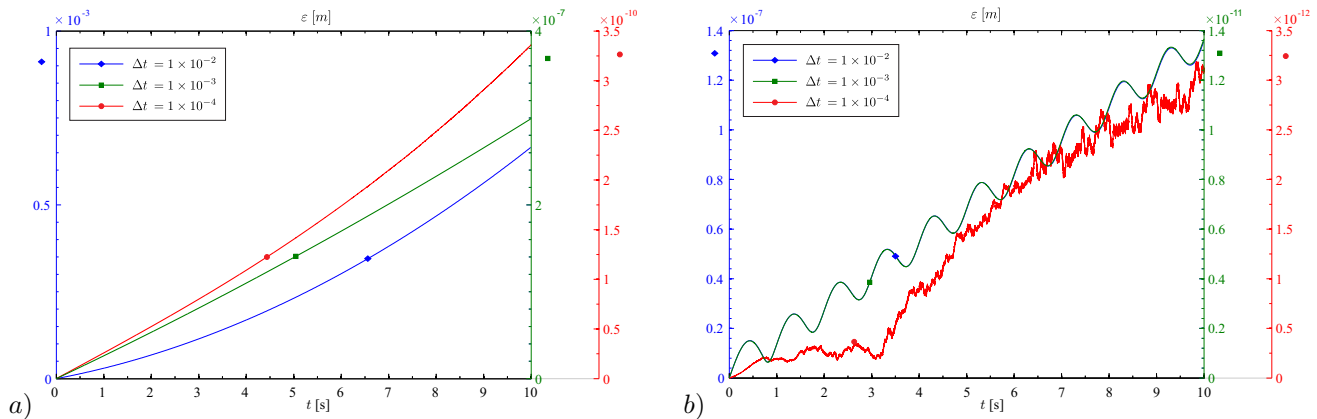


Figure 6. Drift  $\varepsilon$  of the COM from the analytic solution when integrating a) the  $SE(3)$ , and b) the  $SO(3) \times \mathbb{R}^3$  formulation.

### 5.3 Heavy Top

A heavy top is modeled as a rigid body pivoted to the ground at the point  $Q$  as shown in figure 7. The top is suspended by a spring attached to its COM (the geometric center of the box) and a space-fixed point  $P$ . The body-fixed reference frame is located at the COM, which, in the reference configuration, has the same orientation as the shown inertial frame. The pivot point is the center of rotation of the top moving in gravity field.

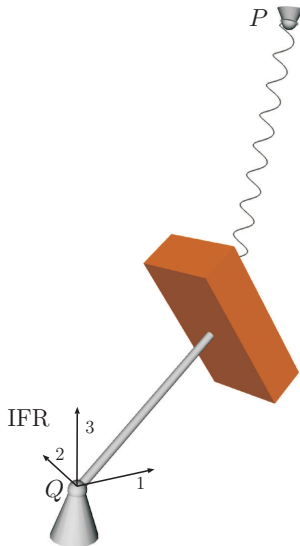


Figure 7. Model of a heavy top consisting of a rigid body, constrained by a massless rod to rotate about a fixed point, suspended with a spring attached to its COM.

The spring is modeled by a linear force law with stiffness  $c = 10$  N/mm. Then, in the spatial representation, the vector of applied forces in (31) is  $\mathbf{F}^s = c(\mathbf{p}_0^s - \mathbf{r}^s) + m\mathbf{g}^s$ , with the gravity vector  $\mathbf{g}^s = (0, 0, -g)$ ,  $g = 9.81$  m/s<sup>2</sup>. Here,  $\mathbf{p}_0^s = (1, 0, 0.5)$  m is the space-fixed position vector of the suspension point  $P$  of the spring. Further, in (31)  $\mathbf{M} = \mathbf{0}$ , since no torques act on the COM. The force vector in the body-fixed representation (28) is  $\mathbf{F} = \mathbf{R}^T \mathbf{F}^s$ .

The body is a solid box with side lengths  $0.1 \times 0.2 \times 0.4$  m made of aluminium. The body has a mass of  $m = 21.6$  kg and its inertia tensor w.r.t. the COM is  $\Theta_0 = \text{diag}(0.36, 0.306, 0.09)$  kg m<sup>2</sup>. The top is constrained to rotate about a fixed point. Denote with  $\mathbf{r}_0 = (-0.5, 0, 0)$  m the position vector of the pivot point measured in the body-fixed reference frame. The configuration of the reference frame is represented by  $C = (\mathbf{R}, \mathbf{r}^s)$ , with rotation matrix  $\mathbf{R}$  and  $\mathbf{r}^s$  denoting the position of the COM expressed in the spatial inertial frame (IFR).

**5.3.1 Motion Equations in Body-Fixed Representation.** The body-fixed twist is denoted  $\mathbf{V} = (\boldsymbol{\omega}, \mathbf{v})$ . The geometric constraints imposed by the spherical joint (pivot) are

$$h(C) = \mathbf{r}^s + \mathbf{R}\mathbf{r}_0 = \mathbf{0}. \quad (25)$$

The time differentiation, and assuming (25), yields the velocity constraints (7)

$$(\hat{\mathbf{r}}_0 - \mathbf{I}) \begin{pmatrix} \boldsymbol{\omega} \\ \mathbf{v} \end{pmatrix} = \mathbf{J}\mathbf{V} = \mathbf{0} \quad (26)$$

and the acceleration constraints

$$(\hat{\mathbf{r}}_0 - \mathbf{I}) \begin{pmatrix} \dot{\boldsymbol{\omega}} \\ \dot{\mathbf{v}} \end{pmatrix} = \hat{\boldsymbol{\omega}}\hat{\boldsymbol{\omega}}\mathbf{r}_0 + \hat{\boldsymbol{\omega}}\mathbf{v}. \quad (27)$$

The body-fixed Newton-Euler equations w.r.t. to the COM combined with (27) yield the overall index 1 DAE system

$$\begin{pmatrix} \Theta_0 & \mathbf{0} & \hat{\mathbf{r}}_0^T \\ \mathbf{0} & m\mathbf{I} & -\mathbf{I} \\ \hat{\mathbf{r}}_0 & -\mathbf{I} & \mathbf{0} \end{pmatrix} \begin{pmatrix} \dot{\boldsymbol{\omega}} \\ \dot{\mathbf{v}} \\ \boldsymbol{\lambda} \end{pmatrix} = \begin{pmatrix} \hat{\boldsymbol{\omega}}\Theta_0\boldsymbol{\omega} \\ \mathbf{F} - m\hat{\boldsymbol{\omega}}\mathbf{v} \\ \hat{\boldsymbol{\omega}}\hat{\boldsymbol{\omega}}\mathbf{r}_0 + \hat{\boldsymbol{\omega}}\mathbf{v} \end{pmatrix}. \quad (28)$$

The vector  $\mathbf{F}$  is the external force acting upon the COM represented in the body-fixed frame.

**5.3.2 Motion Equations in Mixed Velocity Representation.** In the mixed velocity representation  $\mathbf{V}^m = (\boldsymbol{\omega}, \mathbf{v}^s)$ , the geometric constraints (25) gives rise to the following velocity and acceleration constraints, respectively,

$$(\mathbf{R}\hat{\mathbf{r}}_0 - \mathbf{I}) \begin{pmatrix} \boldsymbol{\omega} \\ \mathbf{v}^s \end{pmatrix} = \mathbf{0} \quad (29)$$

$$(\mathbf{R}\hat{\mathbf{r}}_0 - \mathbf{I}) \begin{pmatrix} \dot{\boldsymbol{\omega}} \\ \dot{\mathbf{v}}^s \end{pmatrix} = \mathbf{R}\hat{\boldsymbol{\omega}}\hat{\boldsymbol{\omega}}\mathbf{r}_0. \quad (30)$$

This, together with the Newton-Euler equations w.r.t. to the COM in the mixed representation, yields

$$\begin{pmatrix} \Theta & \mathbf{0} & -\hat{\mathbf{r}}_0\mathbf{R}^T \\ \mathbf{0} & m\mathbf{I} & -\mathbf{I} \\ \mathbf{R}\hat{\mathbf{r}}_0 & -\mathbf{I} & \mathbf{0} \end{pmatrix} \begin{pmatrix} \dot{\boldsymbol{\omega}} \\ \dot{\mathbf{v}}^s \\ \boldsymbol{\lambda} \end{pmatrix} = \begin{pmatrix} -\hat{\boldsymbol{\omega}}\Theta_0\boldsymbol{\omega} \\ \mathbf{F}^s \\ \mathbf{R}\hat{\boldsymbol{\omega}}\hat{\boldsymbol{\omega}}\mathbf{r}_0 \end{pmatrix} \quad (31)$$

where  $\mathbf{F}^s$  is the external force acting upon the COM represented in the spatial inertial frame.

**5.3.3 Numerical Results.** The systems (31) and (28) were integrated for 8 s starting from the initial configuration  $C_0 = (\mathbf{I}, \mathbf{r}_0)$  with the initial velocities  $\boldsymbol{\omega}_0 = (0, 0, 0.5)$  rad/s and  $\mathbf{v}_0 = \mathbf{r}_0 \times \boldsymbol{\omega}_0$ .

Figure 8 reveals that the  $SE(3)$  update preserves the center of rotation with accuracy closed to the computation precision for all three step size values (shown is the error in the translation constraints  $\varepsilon(C) = \|h(C)\|$ ). The  $SO(3) \times \mathbb{R}^3$  formulation on the other hand leads to a significant drift. The difference is clearly visible in the

error of the total energy (starting from  $E(0) = 5000.69$  J) in figure 9. Although the configuration update does not affect the order of accuracy of the overall integration scheme it is also beneficial for the energy conservation.

The pure rotational motion of the top belongs to the rotation group as a  $SE(3)$  subgroup. But since it is not a rotation about the origin of the reference frame (leading to coupled translations), it is not a subgroup of  $SO(3) \times \mathbb{R}^3$ .

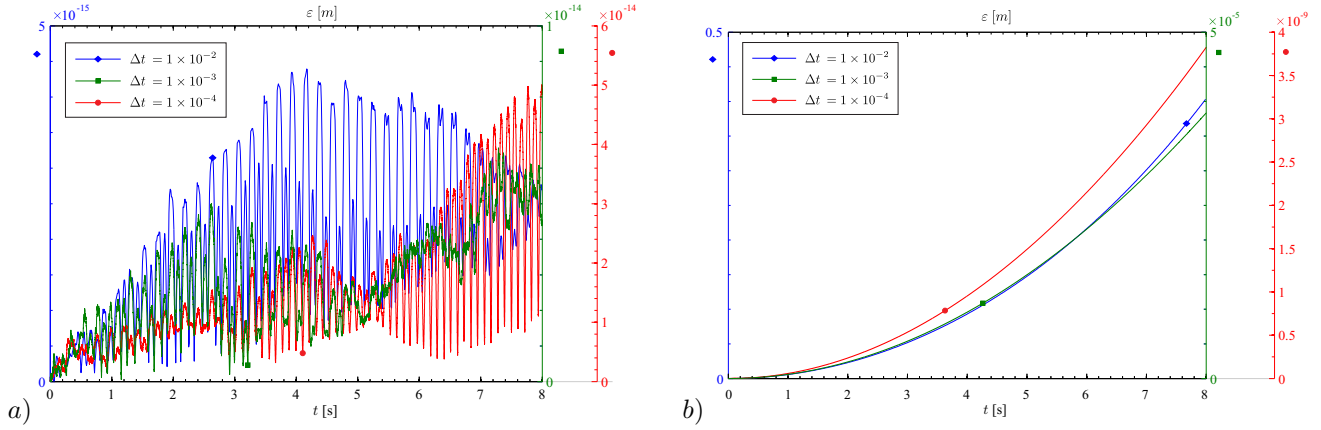


Figure 8. Error  $\varepsilon$  in the position constraints of the top when integrating a) the  $SE(3)$ , and b) the  $SO(3) \times \mathbb{R}^3$  formulation.

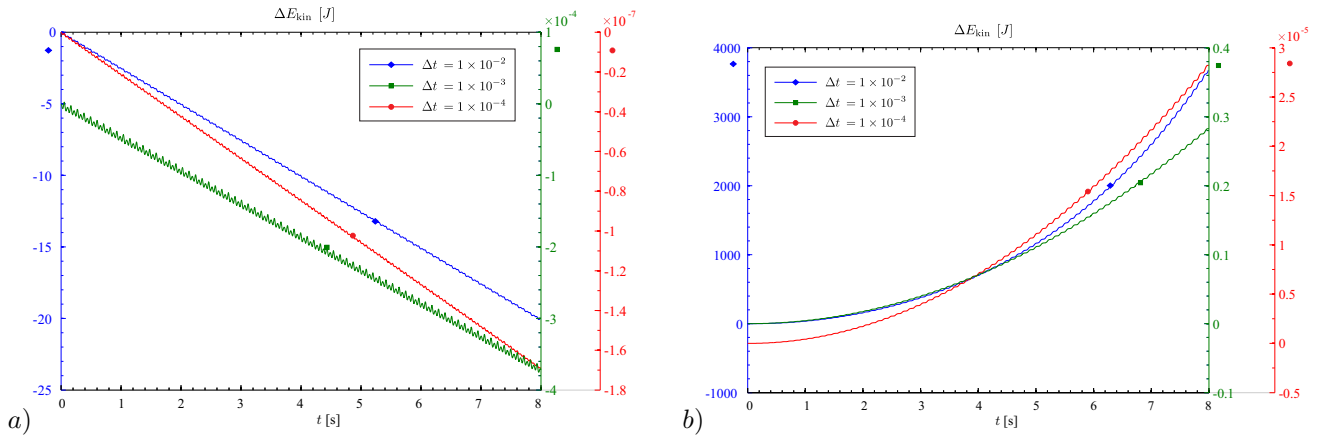


Figure 9. Drift of the the total energy when integrating a) the  $SE(3)$ , and b) the  $SO(3) \times \mathbb{R}^3$  formulation.

#### 5.4 Spherical Double Pendulum in the Gravity Field

The double pendulum as shown in figure 10 consists of the two rigid bodies. The two bodies are interconnected and the pendulum as a whole is connected to the ground by the spherical joints. The two links are flat boxes with the side length  $a, b, c$  along the axes of the COM reference frame. Both have the same dimension with the lengths  $a = 0.2 \text{ m}, b = 0.1 \text{ m}, c = 0.05 \text{ m}$ . Figure 10 shows the inertia ellipsoids. The configuration of the system is represented by  $C_1 = (\mathbf{R}_1, \mathbf{r}_1^s)$  and  $C_2 = (\mathbf{R}_2, \mathbf{r}_2^s)$ . The two links are subject to the geometric constraints

$$\begin{aligned} h_1(C_1) &= \mathbf{R}_1 \mathbf{r}_0 + \mathbf{r}_1^s = \mathbf{0} \\ h_2(C_1, C_2) &= \mathbf{R}_1 \mathbf{r}_{10} + \mathbf{r}_1^s - \mathbf{R}_2 \mathbf{r}_{20} - \mathbf{r}_2^s = \mathbf{0} \end{aligned} \quad (32)$$

where  $\mathbf{r}_{i0}, i = 1, 2$  is the position vector from the COM frame on body  $i$  to the spherical joint connecting the two links, expressed in the COM frame. The variable  $\mathbf{r}_0$  is the position vector from the COM frame on body 1 to the spherical joint connecting it to the ground expressed in this COM frame. Denote with  $\Theta_{i0}$  the inertia tensor of body  $i$  w.r.t. the COM frame, and with  $m_i$  its mass.

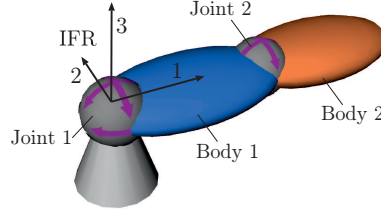


Figure 10. Spherical double pendulum.

**Motion Equations in the Body-Fixed Representation** The velocity and acceleration constraints corresponding to (32), in the terms of the body-fixed twists  $\mathbf{V}_1, \mathbf{V}_2 \in se(3)$ , are

$$\mathbf{0} = \begin{pmatrix} \hat{\mathbf{r}}_0 & -\mathbf{I} & \mathbf{0} & \mathbf{0} \\ \mathbf{R}_1 \hat{\mathbf{r}}_{10} & -\mathbf{R}_1 & -\mathbf{R}_2 \hat{\mathbf{r}}_{20} & \mathbf{R}_2 \end{pmatrix} \begin{pmatrix} \boldsymbol{\omega}_1 \\ \mathbf{v}_1 \\ \boldsymbol{\omega}_2 \\ \mathbf{v}_2 \end{pmatrix} = \mathbf{J}\mathbf{V} \quad (33)$$

$$\mathbf{J}\dot{\mathbf{V}} = -\dot{\mathbf{J}}\mathbf{V}, \text{ with } -\dot{\mathbf{J}}\mathbf{V} = \begin{pmatrix} \hat{\boldsymbol{\omega}}_1 \mathbf{v}_1 + \hat{\boldsymbol{\omega}}_1 \hat{\boldsymbol{\omega}}_1 \mathbf{r}_0 \\ \mathbf{R}_1 \hat{\boldsymbol{\omega}}_1 \hat{\boldsymbol{\omega}}_1 \mathbf{r}_{10} - \mathbf{R}_2 \hat{\boldsymbol{\omega}}_2 \hat{\boldsymbol{\omega}}_2 \mathbf{r}_{20} + \mathbf{R}_1 \hat{\boldsymbol{\omega}}_1 \mathbf{v}_1 - \mathbf{R}_2 \hat{\boldsymbol{\omega}}_2 \mathbf{v}_2 \end{pmatrix}. \quad (34)$$

Using a reference frame at the COM yields

$$\begin{pmatrix} \Theta_{10} & \mathbf{0} & \mathbf{0} & \mathbf{0} & -\hat{\mathbf{r}}_0 & -\hat{\mathbf{r}}_{10} \mathbf{R}_1^T \\ \mathbf{0} & m_1 \mathbf{I} & \mathbf{0} & \mathbf{0} & -\mathbf{I} & -\mathbf{R}_1^T \\ \mathbf{0} & \mathbf{0} & \Theta_{20} & \mathbf{0} & \mathbf{0} & \hat{\mathbf{r}}_{20} \mathbf{R}_2^T \\ \mathbf{0} & \mathbf{0} & \mathbf{0} & m_2 \mathbf{I} & \mathbf{0} & \mathbf{R}_2^T \\ \hat{\mathbf{r}}_0 & -\mathbf{I} & \mathbf{0} & \mathbf{0} & \mathbf{0} & \mathbf{0} \\ \mathbf{R}_1 \hat{\mathbf{r}}_{10} & -\mathbf{R}_1 & -\mathbf{R}_2 \hat{\mathbf{r}}_{20} & \mathbf{R}_2 & \mathbf{0} & \mathbf{0} \end{pmatrix} \begin{pmatrix} \dot{\boldsymbol{\omega}}_1 \\ \dot{\mathbf{v}}_1 \\ \dot{\boldsymbol{\omega}}_2 \\ \dot{\mathbf{v}}_2 \\ \lambda_1 \\ \lambda_2 \end{pmatrix} = \begin{pmatrix} -\hat{\boldsymbol{\omega}}_1 \Theta_{10} \boldsymbol{\omega}_1 \\ \mathbf{F}_1 - m_1 \hat{\boldsymbol{\omega}}_1 \mathbf{v}_1 \\ -\hat{\boldsymbol{\omega}}_2 \Theta_{20} \boldsymbol{\omega}_2 \\ \mathbf{F}_2 - m_2 \hat{\boldsymbol{\omega}}_2 \mathbf{v}_2 \\ * \\ ** \end{pmatrix} \quad (35)$$

where  $*$  and  $**$  are the terms in the two rows of the right hand side of (34). Since only the gravity forces act on the system, the body-fixed forces are  $\mathbf{F}_i = \mathbf{R}_i^T \mathbf{g}^s$ , where  $\mathbf{g}^s = (0, 0, -g)$  is the gravity vector w.r.t. space-fixed frame. The Lagrange multiplier  $\lambda_i \in \mathbb{R}^3$  is the reaction force in the joint  $i$ .

**Motion Equations in the Mixed Velocity Representation** With the mixed velocities  $\mathbf{V}_i^m = (\boldsymbol{\omega}_i, \mathbf{v}_i^s)$ , the velocity and the acceleration constraints are

$$\mathbf{0} = \begin{pmatrix} \mathbf{R}_1 \hat{\mathbf{r}}_0 & -\mathbf{I} & \mathbf{0} & \mathbf{0} \\ \mathbf{R}_1 \hat{\mathbf{r}}_{10} & -\mathbf{I} & -\mathbf{R}_2 \hat{\mathbf{r}}_{20} & \mathbf{I} \end{pmatrix} \begin{pmatrix} \boldsymbol{\omega}_1 \\ \mathbf{v}_1 \\ \boldsymbol{\omega}_2 \\ \mathbf{v}_2 \end{pmatrix} = \mathbf{J}\mathbf{V}^m \quad (36)$$

$$\mathbf{J}\dot{\mathbf{V}}^m = -\dot{\mathbf{J}}\mathbf{V}^m, \text{ with } -\dot{\mathbf{J}}\mathbf{V}^m = \begin{pmatrix} \mathbf{R}_1 \hat{\boldsymbol{\omega}}_1 \hat{\boldsymbol{\omega}}_1 \mathbf{r}_0 \\ \mathbf{R}_1 \hat{\boldsymbol{\omega}}_1 \hat{\boldsymbol{\omega}}_1 \mathbf{r}_{10} - \mathbf{R}_2 \hat{\boldsymbol{\omega}}_2 \hat{\boldsymbol{\omega}}_2 \mathbf{r}_{20} \end{pmatrix}. \quad (37)$$



The DAE index 1 motion equations are, with the force vectors  $\mathbf{F}_i^s = \mathbf{g}^s$ ,

$$\begin{pmatrix} \Theta_{10} & \mathbf{0} & \mathbf{0} & \mathbf{0} & -\hat{\mathbf{r}}_0 \mathbf{R}_1^T & -\hat{\mathbf{r}}_{10} \mathbf{R}_1^T \\ \mathbf{0} & m_1 \mathbf{I} & \mathbf{0} & \mathbf{0} & -\mathbf{I} & -\mathbf{I} \\ \mathbf{0} & \mathbf{0} & \Theta_{20} & \mathbf{0} & \mathbf{0} & \hat{\mathbf{r}}_{20} \mathbf{R}_2^T \\ \mathbf{0} & \mathbf{0} & \mathbf{0} & m_2 \mathbf{I} & \mathbf{0} & \mathbf{I} \\ \mathbf{R}_1 \hat{\mathbf{r}}_0 & -\mathbf{I} & \mathbf{0} & \mathbf{0} & \mathbf{0} & \mathbf{0} \\ \mathbf{R}_1 \hat{\mathbf{r}}_{10} & -\mathbf{I} & -\mathbf{R}_2 \hat{\mathbf{r}}_{20} & \mathbf{I} & \mathbf{0} & \mathbf{0} \end{pmatrix} \begin{pmatrix} \dot{\boldsymbol{\omega}}_1 \\ \dot{\mathbf{v}}_1^s \\ \boldsymbol{\omega}_2 \\ \dot{\mathbf{v}}_2^s \\ \boldsymbol{\lambda}_1 \\ \boldsymbol{\lambda}_2 \end{pmatrix} = \begin{pmatrix} -\hat{\boldsymbol{\omega}}_1 \Theta_{10} \boldsymbol{\omega}_1 \\ \mathbf{F}_1^s \\ -\hat{\boldsymbol{\omega}}_2 \Theta_{20} \boldsymbol{\omega}_2 \\ \mathbf{F}_2^s \\ * \\ ** \end{pmatrix}$$

The terms \* and \*\* are the two rows entries at the right hand side of (37).

**Numerical Results** In the initial configuration  $C_1(0) = (\mathbf{I}, (a_1/2, 0, 0))$ ,  $C_2(0) = (\mathbf{I}, (a_1 + a_2/2, 0, 0))$  the pendulum is aligned with the space-fixed x-axis as shown in figure 10. The pendulum is moving in the gravity field with the initial velocities set to  $\boldsymbol{\omega}_{10} = (10, 0, 0)$  rad/s and  $\boldsymbol{\omega}_{20} = (10\pi, 10\pi, 20\pi)$  rad/s.

The figure 11a) shows the exact constraint satisfaction up to the computation precision for joint 1 for  $SE(3)$ . Both formulations achieve a similar constraint satisfaction for joint 2 (figure 12). The joint 1 constrains the body 1 to perform the rotational motion, i.e. to a subgroup of  $SE(3)$ . Thus, the condition of the corollary 1 is satisfied. Overall, the  $SE(3)$  update performs best as concluded in corollary 1 (for joint 1) and 3 (for joint 2).

The constraint violation is also reflected in the drift of the total energy in figure 13 that becomes significant for the  $SO(3) \times \mathbb{R}^3$  update with the large step size. Similar results were obtained for a spherical three-bar and a four-bar pendulum.

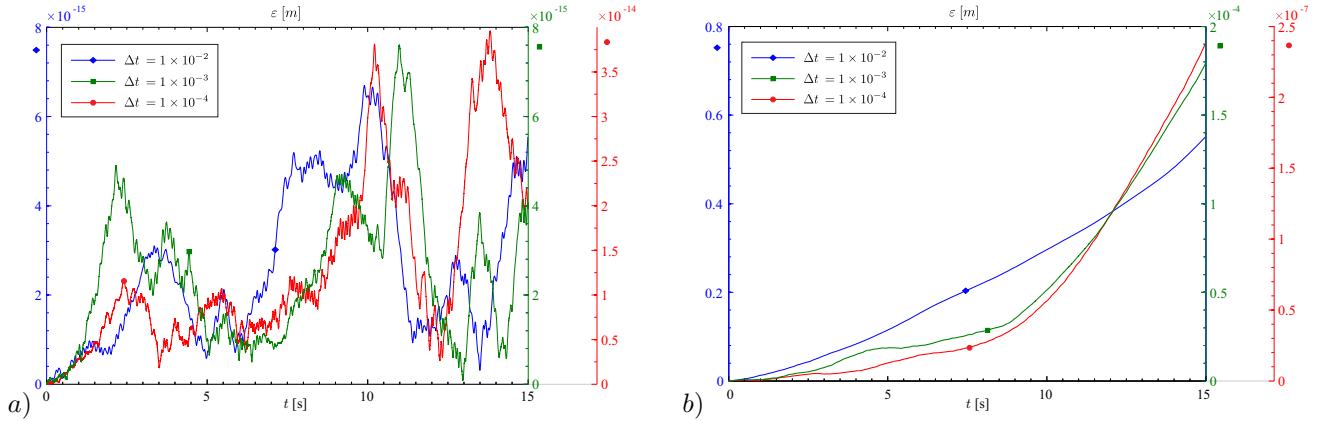


Figure 11. Violation of geometric constraints of joint 1 when integrating the  $SE(3)$  (a), and  $SO(3) \times \mathbb{R}^3$  (b) formulation.

## 5.5 Planar 4-Bar Mechanism

The closed loop planar 4-bar mechanism in figure 14 consists of the three rigid bodies linked to the ground. Body 1, 2, and 3 are mutually connected with the revolute joints. Furthermore, the bodies 1 and 3 are connected

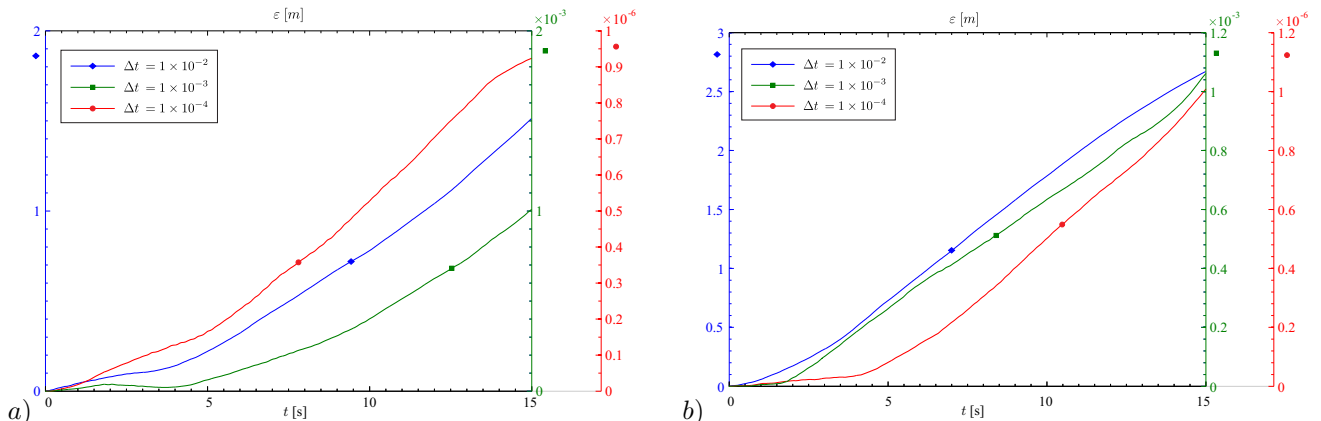


Figure 12. Violation of geometric constraints of joint 2 when integrating a) the  $SE(3)$ , and b)  $SO(3) \times \mathbb{R}^3$  formulation.

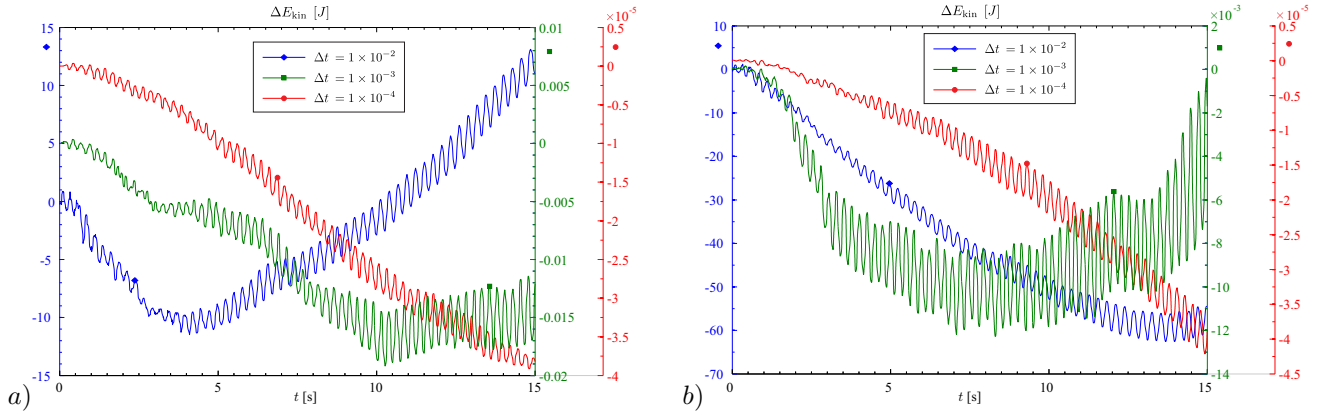


Figure 13. Drift of total energy for a) the  $SE(3)$ , and b)  $SO(3) \times \mathbb{R}^3$  update.

to the ground by the revolute joints. The motion equations are omitted for the sake of the brevity. The geometric parameters are indicated in figure 14, and  $L_0 = 0.5$  m is used in the simulations.

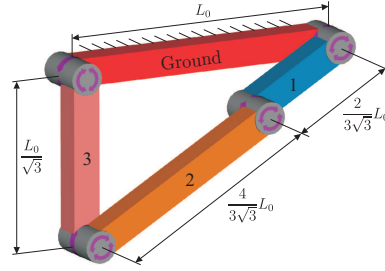


Figure 14. Planar 4-bar mechanism comprising four revolute joints with parallel axes.

The initial configuration is shown in figure 14. The initial velocities are set in the way that the input crank (body 1) rotates with the angular velocity  $\omega_0 = 10 \pi$  rad/s. Thus the motion equations were integrated with the initial conditions  $\omega_{10} = (0, 0, \omega_0)$ ,  $\omega_{20} = (0, 0, -\omega_0/2)$ ,  $\omega_{30} = (0, 0, 0)$ ,  $\mathbf{v}_{10} = (L_0\omega_0/(3\sqrt{3}), 0, 0)$ ,  $\mathbf{v}_{20} = (0, 2L_0\omega_0/(3\sqrt{3}), 0, 0)$ ,  $\mathbf{v}_{30} = (0, 0, 0)$ . The numerical results are shown in figures 15 and 16. The orientation constraints are exactly satisfied by the both formulations. This example confirms again the statement that the  $SE(3)$  update exactly preserves the lower pair constraints restricting the body 1 and 3 to a subgroup (corollary 1), and also that the joint constraints are exactly satisfied (lemma 2). In this example, the bodies 1 and 3 are constrained so to perform the rotational motion about a constant axis.

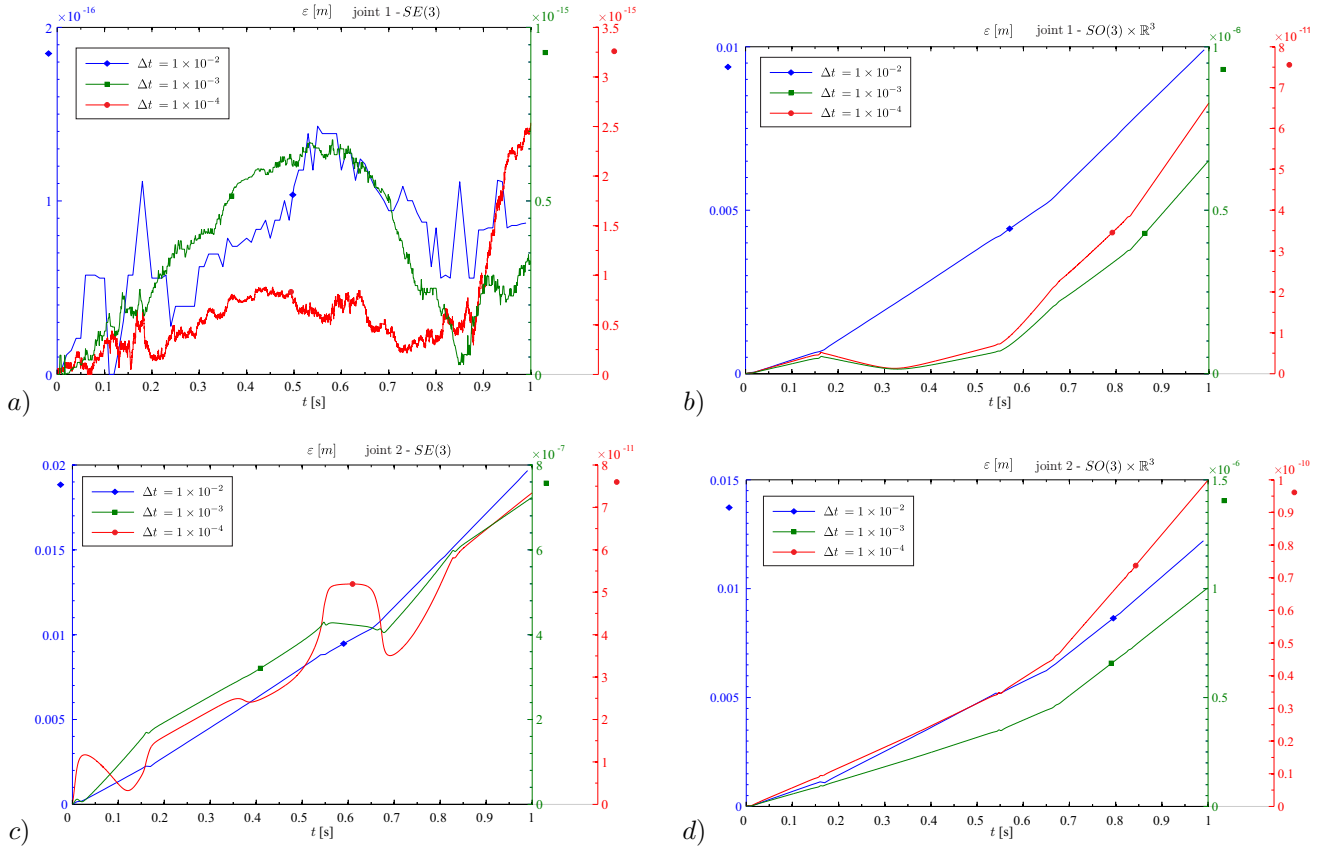


Figure 15. Violation of geometric constraints of revolute joint 1 and 2 when integrating a,c) the  $SE(3)$ , and b,d) the  $SO(3) \times \mathbb{R}^3$  formulation.

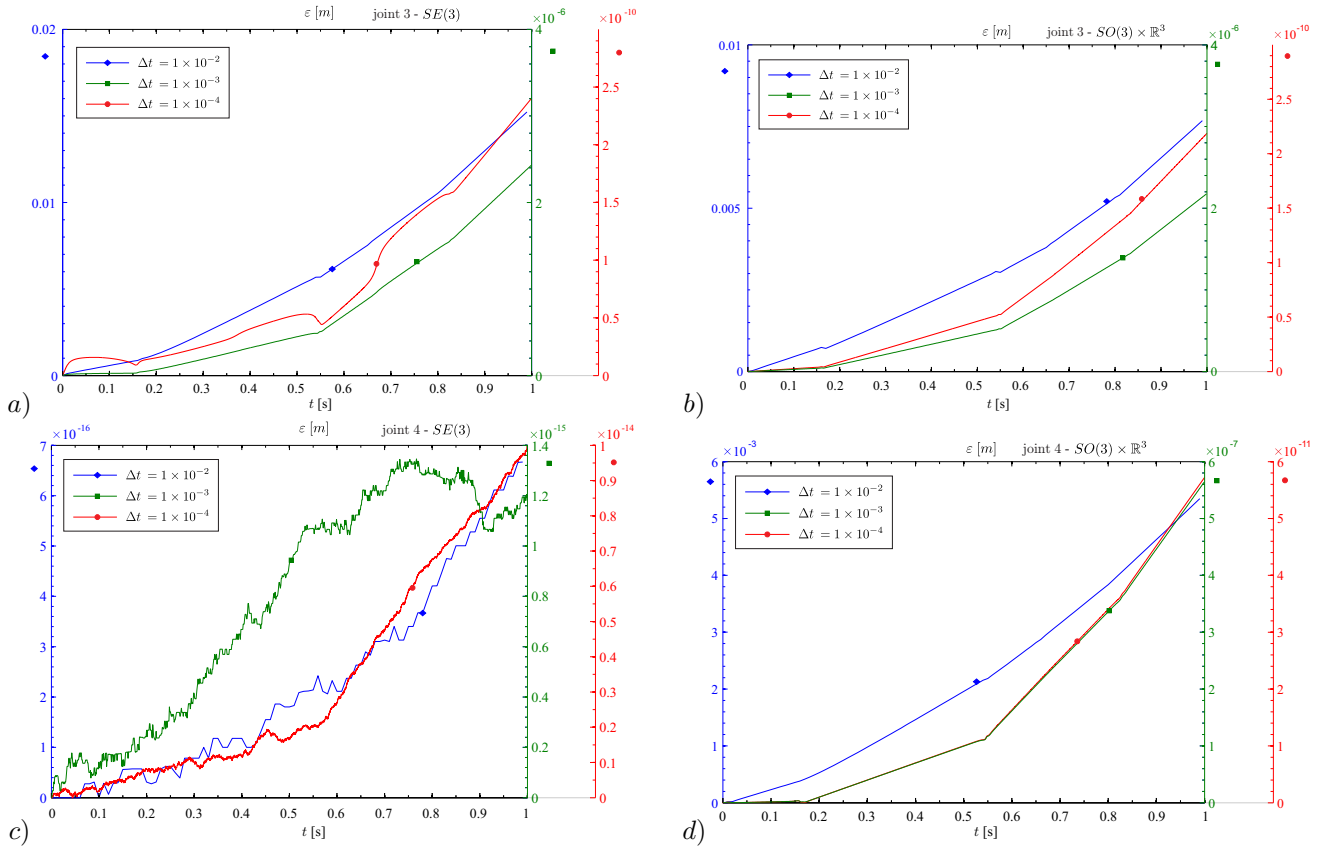


Figure 16. Violation of geometric constraints of revolute joint 3 and spherical joint 4 when integrating a,c) the  $SE(3)$ , and b,d) the  $SO(3) \times \mathbb{R}^3$  formulation.

## 5.6 RP Mechanisms

As next example, the mechanism in figure 17 is considered consisting of a cylindrical ring (body 1) connected to the ground by a revolute joint 1 and to another body (body 2) by a prismatic joint 2. The two bodies are elastically coupled by a longitudinal spring along the prismatic joint. The system is moving in the gravity field as indicated in figure 17 with the gravity vector  $\mathbf{g}^s = (0, 0, -9.81) \text{ m/s}^2$ . By assuming that material is aluminium, the respective mass is  $m_1 = 6.82825 \text{ kg}$  and  $m_2 = 0.864 \text{ kg}$ . The inertia matrix of body 1 and 2, w.r.t. the body-fixed reference frames at the COM, is  $\Theta_1 = \text{diag}(0.0507567, 0.0507567, 0.0986682) \text{ kg m}^2$  and  $\Theta_2 = \text{diag}(0.0002304, 0.0029952, 0.0029952) \text{ kg m}^2$ , respectively. The dynamics of the bodies is governed by the Newton-Euler equations supplemented by the joint constraints (not shown here for the sake of brevity). The spring stiffness is set to  $10^4 \text{ N/m}$ .

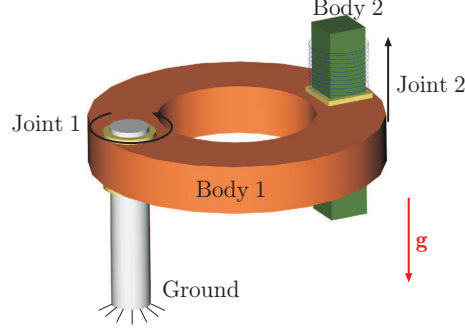


Figure 17. RP kinematic chain: Two bodies connected by a prismatic joint 2, and connected to the ground by revolute joint 1.

The motion equations are integrated with the initial conditions  $\boldsymbol{\omega}_{10} = \boldsymbol{\omega}_{20} = (0, 0, 20\pi) \text{ rad/s}$  and  $\mathbf{v}_{10} = \mathbf{r}_1 \times \boldsymbol{\omega}_{10}$ ,  $\mathbf{v}_{20} = \mathbf{r}_{21} \times \boldsymbol{\omega}_{20} + (0, 0, 1) \text{ m/s}$ , where  $\mathbf{r}_{1i}$  is the position vector of the axis of joint 1 w.r.t. to the COM frame on the body  $i$ . That is, the prismatic joint 2 is given an initial velocity of 1 m/s.

The numerical results in figure 18a) and 19a) show the constraint satisfaction, indicating an excellent motion reconstruction, when the  $SE(3)$  update is used. Using the  $SO(3) \times \mathbb{R}^3$  formulation yields the accuracy depending on the integration step size as shown in figures 18b) and 19b). This is an example where lemma 2 applies. Both bodies are free to move in a  $SE(3)$  subgroup and the actions of the revolute and prismatic joint commute. The body 1 performs a pure rotational motion (subgroup  $SO(2)$ ) and the body 2 a 'cylindrical' motion, i.e. a rotation about a fixed axis plus a translation along this axis (subgroup  $SO(2) \times \mathbb{R}$ ). The same accuracy is achieved when the joint 1 is a cylindrical joint. Note again that the step size can be arbitrarily large and the  $SE(3)$  update still satisfies the kinematic joint constraints.

Using  $SO(3) \times \mathbb{R}^3$  as c-space, the motion space of body 1 is only a submanifold of the subgroup  $SO(2) \times \mathbb{R}^2$  of the c-space, and the motion space of the body 2 is a submanifold of the c-space subgroup  $SO(2) \times \mathbb{R}^3$ , thus this update cannot satisfy the joint constraints.

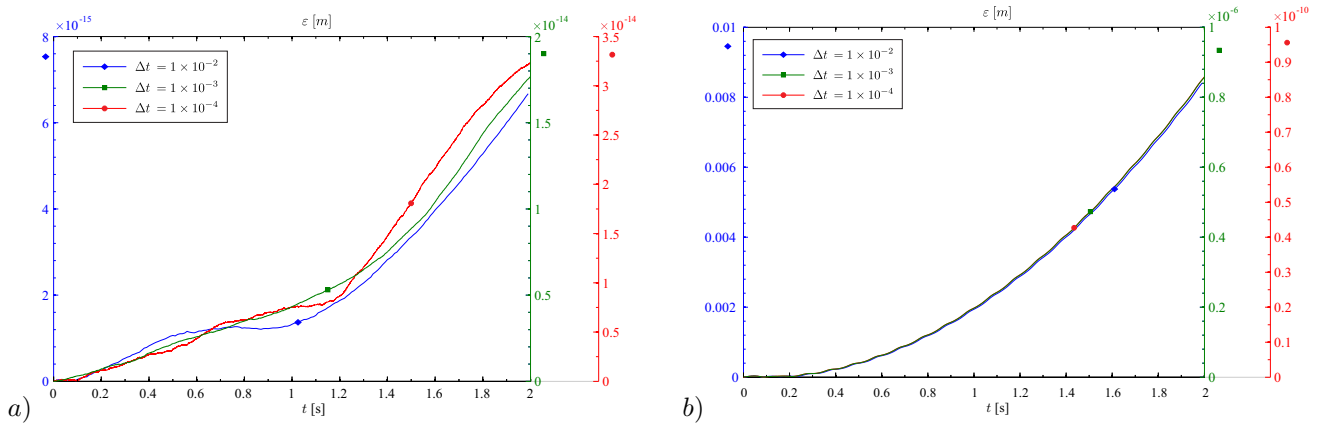


Figure 18. Violation of geometric constraints of revolute joint 1 when integrating a) the  $SE(3)$ , and b)  $SO(3) \times \mathbb{R}^3$  formulation.

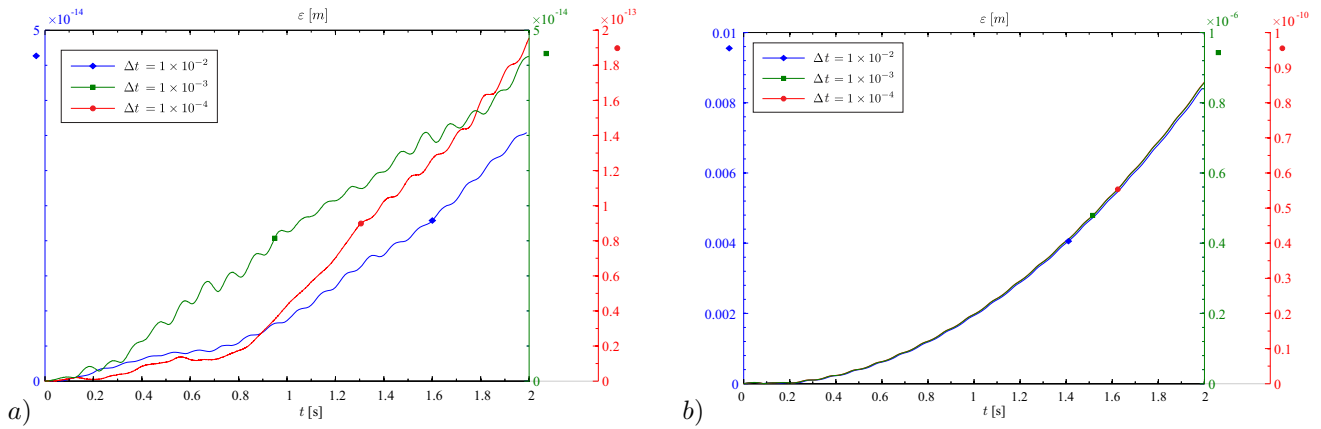


Figure 19. Violation of geometric constraints of prismatic joint 2 when integrating a) the  $SE(3)$ , and b)  $SO(3) \times \mathbb{R}^3$  formulation.

## 5.7 Cardanic Transmission

The last example is a Cardanic transmission presented in figure 20. The input shaft (body 1), mounted at the ground by a revolute joint (joint 1), is connected to a drive shaft (body 2) by a universal joint (joint 2). In this example, the body 1 is constrained to perform rotation about the fixed axis of the revolute joint 1. Since the reference (COM) frame of the body 1 is located at the rotation axis of the revolute joint, there is no translation component. Hence, the motion observed at this point is a pure rotation and the both formulations yield a perfect constraint satisfaction (otherwise  $SO(3) \times \mathbb{R}^3$  would not). The motion equations are integrated with initial velocities  $\omega_1 = (0, \pi, 0)$  rad/s, and  $\omega_2 = (\pi, \pi, 0)$  rad/s. In the initial configuration the two bodies are aligned along the 3-axis.

The universal joint connecting body 1 and body 2 adds two rotational degrees of freedom (DOF) so that body 2 is constrained to perform free spatial rotations about the intersection point of the two hook joint axes. The combination of the two joints is equivalent to a spherical joint constraining the reference frame on body 2 to move on a sphere centered at the hook joint. That is, body 2 is constrained to the subgroup  $SO(3)$  of  $SE(3)$ . Due to the translation components, the motion does, however, not form a subgroup of  $SO(3) \times \mathbb{R}^3$ . The condition of corollary 1 is thus fulfilled for the  $SE(3)$  update only. Consequently, the position constraints of the joint 2 should be perfectly satisfied. This is confirmed in figure 21a). This is not so for the  $SO(3) \times \mathbb{R}^3$  update as shown in figure 21b).

The hook joint does not define a subgroup of  $SE(3)$  or  $SO(3) \times \mathbb{R}^3$  so that the condition of lemma 2 is not satisfied. Therefore, the orientation constraints of the hook joint are not exactly satisfied, but only according to the time step size and order of accuracy of the RK4 integration method. This is documented in figure 22 revealing the same constraint satisfaction of both configuration update variants.

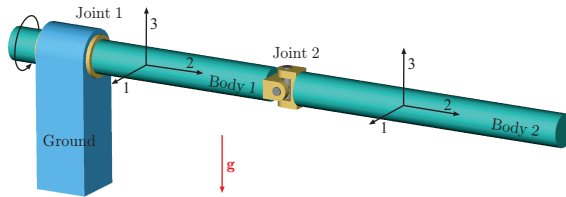


Figure 20. A Cardanic transmission consisting of an input shaft (body 1), mounted at the ground by a revolute joint 1, connected to the drive shaft (body 2) by a universal joint 2.

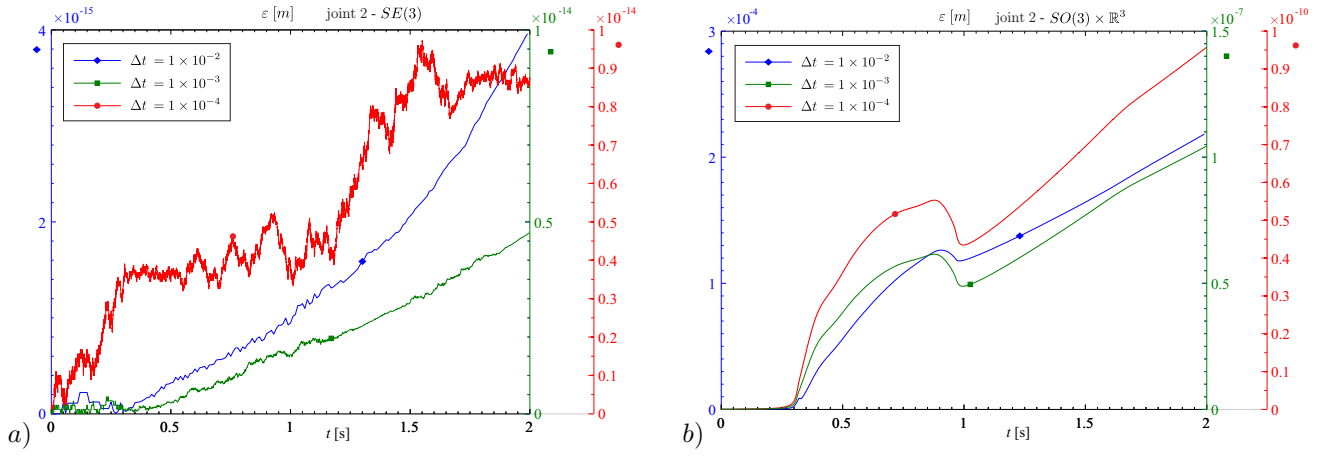


Figure 21. Violation of position constraints of universal joint 2 when integrating a) the  $SE(3)$ , and b)  $SO(3) \times \mathbb{R}^3$  formulation.

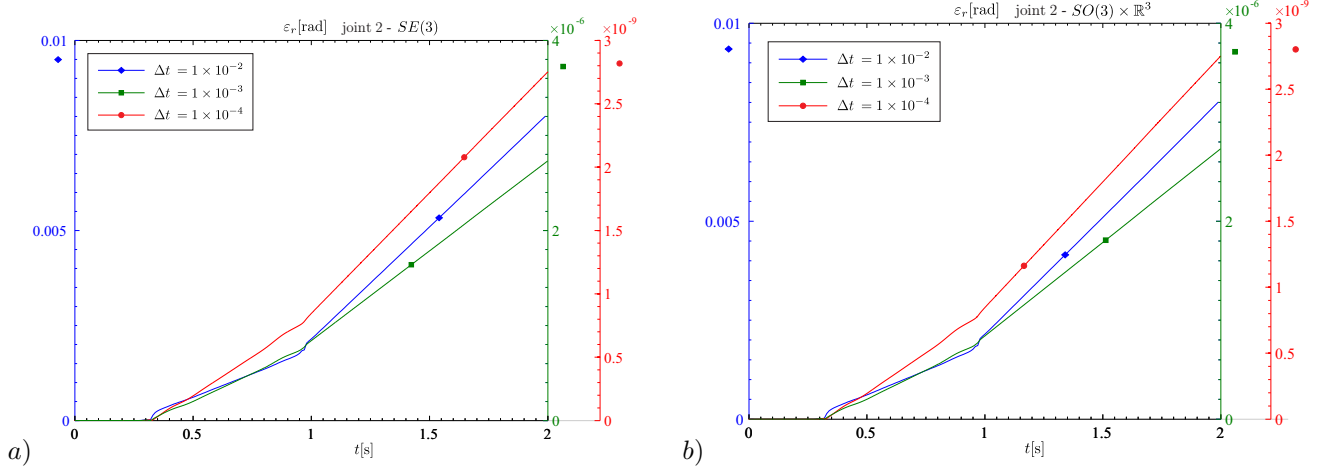


Figure 22. Violation of orientation constraints of universal joint 2 when integrating a) the  $SE(3)$ , and b)  $SO(3) \times \mathbb{R}^3$  formulation.

## 6 Discussion and Conclusion

The dynamics of a constrained MBS comprising rigid bodies is governed by the Newton-Euler equations (1a) together with the kinematic reconstruction equations (1b). The latter reveal the actual motion of the MBS corresponding to its velocity. Moreover, in a numerical integration scheme these are used to estimate finite motion increments. Since (1b) respectively (14b), (15b), and (17b), reflect the geometry of the c-space Lie group, a different c-space leads to different numerical results. This has a consequence for the constraint satisfaction when (1) is replaced by the index 1 systems of the form (14), (15), or (17) and is solved with the ODE integrators. While the accuracy of the numerical solution of the ODE is determined by the integration method, the geometric constraints should be perfectly satisfied, i.e. the MBS as a whole shall remain assembled. This poses the question, if, and under which conditions, an integration scheme, solving the ODE, can inherently satisfy the constraints independently of its order of accuracy.

Taking a kinematic perspective it was shown in this paper that this issue is connected with the particular form of the kinematic reconstruction equations, i.e. the c-space Lie group, rather than with the integration scheme. The two relevant c-space Lie groups are  $SE(3)$  and  $SO(3) \times \mathbb{R}^3$ . The latter is commonly used (at least implicitly) in modeling of rigid body MBS, whereas the importance of using  $SE(3)$  for the finite element integration schemes has already been recognized [8, 9, 10, 11, 13]. The analysis is facilitated by a general formulation of the motion equations accounting for a general c-space Lie group. For completeness, the Lie groups  $SE(3)$  and  $SO(3) \times \mathbb{R}^3$  are also related to the dual quaternion formulation and the Euler parameter formulation that are frequently used in the applications. The actual motion equations are formulated as a vector space ODE as well as an ODE on the c-space Lie group.

It was shown in section 4 that, if a body is constrained to a subgroup of its c-space Lie group, the corresponding configuration update always yields a body configuration within that subgroup, thus satisfies the *motion constraints imposed on the body*, independently of the actual integration accuracy. On the contrary, when the

motion of a rigid body within the MBS is not constrained to a subgroup, but to an arbitrary submanifold, the update step can lead out of that submanifold and thus violate the constraints. This conclusion does not immediately account for the satisfaction of the joint constraints.

It is known that  $SE(3)$  is the proper Lie group of rigid body motions. But it is shown that this only implies better constraint satisfaction for special MBS. Since subgroups of  $SE(3)$  account for lower pair joints (Reuleaux pairs), an immediate consequence is that the  $SE(3)$  update achieves a perfect satisfaction of the *joint constraints* when a rigid body is connected to the ground by a lower pair joint. Another result is that the lower pair joint constraints are exactly satisfied if the joint connects two bodies that are respectively constrained to a  $SE(3)$  subgroup. The subgroups of the direct product group  $SO(3) \times \mathbb{R}^3$ , which is assumed by the standard form (2), account for situations with a less practical relevance. As such, a prominent example is the free floating body (section 5.1) with the reference frame located at its COM, where the momentum conservation constrains the body to rotate while moving on a straight line. This motion belongs to a subgroup of  $SO(3) \times \mathbb{R}^3$  but not of  $SE(3)$ .

Numerical results are presented in section 5 confirming the above conclusion. The results show that in the general cases, where the constrained motions do not form a subgroup of either c-space Lie group, both  $SE(3)$  and  $SO(3) \times \mathbb{R}^3$  lead to the same order of accuracy. Hence,  $SE(3)$  is superior only for a special class of MBS. Nevertheless, it allows for the construction of tailored simulation models. Since  $SE(3)$  can achieve exact constraint satisfaction for certain MBS comprising lower pair joints, and since for a general MBS the  $SE(3)$  and  $SO(3) \times \mathbb{R}^3$  update scheme yield the same order of accuracy, it can be concluded that  $SE(3)$  is the best choice for a c-space Lie group. From the computational point, however, the expressions (56) and (58) used in the  $SE(3)$  update are slightly more complex than (68). In order to minimize the overall complexity while ensuring the exact constraint satisfaction whenever possible, a c-space Lie group can be tailored to a specific model.

Notice that the c-space only affects the kinematic equations (1b) but not the motion equations (1a) or the integration scheme. From the practical point of view, the question about the c-space boils down to the appropriate configuration update since the c-space is merely a conceptual construct. All said is equally valid for the Euler parameters and dual quaternions as well as for any 3-angle parameterization.

Finally, it should be remarked that the presented results are relevant in general since any DAE formulation (index 1, 2, or 3) of MBS in terms of the non-holonomic velocities involves the kinematic reconstruction equations (1b).

## APPENDIX

### A Geometric Background on Rigid Body Motions

#### A.1 Spatial Rotation

The relative orientation of two frames can be represented by a rotation matrix  $\mathbf{R} \in SO(3)$ . The special orthogonal group  $SO(3)$  is the Lie group of  $3 \times 3$  orthogonal matrices with corresponding Lie algebra  $so(3)$  the vector space of skew symmetric  $3 \times 3$  matrices. The latter is isomorphic to  $\mathbb{R}^3$  via  $\mathbf{x} \in \mathbb{R}^3 \mapsto \widehat{\mathbf{x}} \in so(3)$ , where  $\widehat{\mathbf{x}}$  is the cross product matrix associated to  $\mathbf{x}$ . A rotation can be associated an instantaneous rotation vector  $\boldsymbol{\xi} \in \mathbb{R}^3$ . The finite rotation, i.e. the rotation matrix, corresponding to the (generally not constant rotation vector) is given by the exponential mapping

$$\exp \widehat{\boldsymbol{\xi}} = \mathbf{I} + \frac{\sin \|\boldsymbol{\xi}\|}{\|\boldsymbol{\xi}\|} \widehat{\boldsymbol{\xi}} + \frac{1 - \cos \|\boldsymbol{\xi}\|}{\|\boldsymbol{\xi}\|^2} \widehat{\boldsymbol{\xi}}^2. \quad (38)$$

This is the Euler-Rodriguez formula describing the rotation about the rotation axis  $\boldsymbol{\xi}/\|\boldsymbol{\xi}\|$  by the angle  $\|\boldsymbol{\xi}\|$ .

Since  $so(3)$  is isomorphic to  $\mathbb{R}^3$  with the cross product as Lie bracket, the Lie bracket  $[\widehat{\mathbf{x}}, \widehat{\mathbf{y}}] = \widehat{\mathbf{x}\mathbf{y}} - \widehat{\mathbf{y}\mathbf{x}} = \widehat{\mathbf{x} \times \mathbf{y}}$  on  $so(3)$  is expressed in vector notation as  $[\mathbf{x}, \mathbf{y}] = \widehat{\mathbf{x}\mathbf{y}} = \mathbf{x} \times \mathbf{y}$ .

Expressing the angular velocity in terms of the time derivative of the rotation vector requires the differential of the exp mapping (38). As for any Lie group this is introduced as  $\text{dexp} : so(3) \times so(3) \rightarrow so(3)$ , via right translation so that  $\text{dexp}_{\widehat{\boldsymbol{\xi}}} \dot{\boldsymbol{\xi}} = \dot{\mathbf{R}}\mathbf{R}^{-1}$ , with  $\mathbf{R} = \exp \widehat{\boldsymbol{\xi}}$ . It admits the series expansion

$$\text{dexp}_{\widehat{\boldsymbol{\xi}}}(\widehat{\mathbf{y}}) = \sum_{i \geq 0} \frac{1}{(i+1)!} \text{ad}_{\widehat{\boldsymbol{\xi}}}^i(\widehat{\mathbf{y}}) \quad (39)$$

where  $\text{ad}_{\hat{\mathbf{x}}}(\hat{\mathbf{y}}) = [\hat{\mathbf{x}}, \hat{\mathbf{y}}]$ . With vector notation  $\mathbf{ad}_{\hat{\mathbf{x}}}\hat{\mathbf{y}} = \hat{\mathbf{x}}\mathbf{y}$  this leads to the closed form matrix expressions

$$\mathbf{dexp}_{\xi} = \mathbf{I} + \frac{1 - \cos \|\xi\|}{\|\xi\|^2} \hat{\xi} + \frac{\|\xi\| - \sin \|\xi\|}{\|\xi\|^3} \hat{\xi}^2 \quad (40)$$

$$= \frac{1}{\|\xi\|^2} [(\mathbf{I} - \exp \hat{\xi}) \hat{\xi} + \xi \xi^T]. \quad (41)$$

This matrix is frequently called tangent operator of rotations [65]. Its significance is that it allows for expressing the body-fixed angular velocity in terms of the time derivative of the rotation vector since

$$\boldsymbol{\omega} = \mathbf{dexp}_{-\xi} \dot{\xi} \quad (42)$$

where the left Poisson equation  $\hat{\boldsymbol{\omega}} := \mathbf{R}^T \dot{\mathbf{R}}$  defines the body-fixed angular velocity vector  $\boldsymbol{\omega}$ . Equally important is the inverse relation. The inverse of the  $\mathbf{dexp}$  mapping possesses the expansion

$$\mathbf{dexp}_{\hat{\mathbf{x}}}^{-1}(\hat{\mathbf{y}}) = \sum_{i \geq 0} \frac{B_i}{i!} \text{ad}_{\hat{\mathbf{x}}}^i(\hat{\mathbf{y}}) \quad (43)$$

with  $B_i$  being the Bernoulli numbers. The inverse of (40) is explicitly

$$\mathbf{dexp}_{\xi}^{-1} = \mathbf{I} - \frac{1}{2} \hat{\xi} + \left(1 - \frac{\|\xi\|}{2} \cot \frac{\|\xi\|}{2}\right) \frac{\hat{\xi}^2}{\|\xi\|^2}. \quad (44)$$

This expression seems to have first appeared in [22]. For numerical implementations the second-order approximation of (43)

$$\mathbf{dexp}_{\hat{\mathbf{x}}}^{-1}(\hat{\mathbf{y}}) \approx \hat{\mathbf{y}} - \frac{1}{2} \text{ad}_{\hat{\mathbf{x}}}(\hat{\mathbf{y}}) + \frac{1}{12} \text{ad}_{\hat{\mathbf{x}}}^2(\hat{\mathbf{y}}) \quad (45)$$

can be used. Interestingly, since  $B_3 = 0$ , this is also the third-order approximation. Moreover, since  $B_i = 0$  for odd  $i$ , the approximation of order  $2i$  and  $2i + 1$  are identical. Application of higher order approximations is, however, not advisable as the computational complexity exceeds that of the closed form (44).

## A.2 Proper Rigid Body Motions and Body-Fixed Twists

A rigid body is kinematically represented by a body-fixed reference frame. Its configuration with respect to a world-fixed inertial reference frame is described by the position vector  $\mathbf{r} \in \mathbb{R}^3$  of its origin and the relative rotation matrix  $\mathbf{R} \in SO(3)$ . The *configuration* of a rigid body is thus represented by the pair  $C = (\mathbf{R}, \mathbf{r})$ , and a rigid body motion is a curve  $C(t)$ . The set of such pairs may hence be regarded as the rigid body configuration space. In order to capture the rigid body kinematics this set must be equipped with slightly more structure. This structure has to do with the transition from one configuration to another. The combination of two successive rigid-body configurations is given by  $C_2 \cdot C_1 = (\mathbf{R}_2 \mathbf{R}_1, \mathbf{r}_2 + \mathbf{R}_2 \mathbf{r}_1)$ . The rigid body configurations equipped with this multiplication describes frame transformations, i.e. finite rigid body *motions* that constitute the 6-dimensional Lie group  $SE(3) = SO(3) \times \mathbb{R}^3$  –the special Euclidian group in 3 dimensions, i.e. the group of isometric orientation preserving transformations of 3-dimensional Euclidian spaces. It is crucial to note that this is the *semidirect* product of the special orthogonal group  $SO(3)$  and the translation group, represented by  $\mathbb{R}^3$ , hence the above multiplication law. This is also encoded in the  $4 \times 4$  matrix representation of a rigid body motion

$$\mathbf{C} = \begin{pmatrix} \mathbf{R} & \mathbf{r} \\ \mathbf{0} & 1 \end{pmatrix}. \quad (46)$$

All matrices of the form (46) constitute the representation of  $SE(3)$  as a matrix group, denoted as  $\mathbf{C} \in SE(3)$ . The group multiplication, i.e. the concatenation of two rigid body motions, is then given by the matrix product

$$\mathbf{C}_2 \mathbf{C}_1 = \begin{pmatrix} \mathbf{R}_2 \mathbf{R}_1 & \mathbf{r}_2 + \mathbf{R}_2 \mathbf{r}_1 \\ \mathbf{0} & 1 \end{pmatrix}. \quad (47)$$



To emphasize that  $C \in SE(3)$  represent frame transformations they are occasionally termed 'proper rigid body motions'. A general motion of a rigid body is a screw motion, i.e. an interconnected rotation and translation along a screw axis. The velocity corresponding to the screw motion of a rigid body is a twist characterized by the angular velocity  $\boldsymbol{\omega}$  and the linear velocity vector  $\mathbf{v}$ , both expressed in the body-fixed frame, summarized in the twist coordinate vector  $\mathbf{V} = (\boldsymbol{\omega}, \mathbf{v}) \in \mathbb{R}^6$ . Given a rigid body motion  $\mathbf{C}(t)$ , the twist of the body in body-fixed representation is defined as

$$\widehat{\mathbf{V}} := \mathbf{C}^{-1} \dot{\mathbf{C}} \quad \text{with} \quad \widehat{\mathbf{V}} = \begin{pmatrix} \widehat{\boldsymbol{\omega}} & \mathbf{v} \\ \mathbf{0} & 0 \end{pmatrix} \in se(3) \quad (48)$$

where  $\mathbf{v} = \mathbf{R}^T \dot{\mathbf{r}}$ , and the matrix is given in terms of the twist coordinate vector. Twists are interpreted as instantaneous screws. A general screw coordinate vector is denoted as  $\mathbf{X} = (\boldsymbol{\xi}, \boldsymbol{\eta}) \in \mathbb{R}^6$ . The vector space of matrices of the form (48) forms the matrix representation of the Lie algebra  $se(3)$ , that is the algebra of screws. The hat operator  $\widehat{\cdot}$  is used interchangeably to produce either  $so(3)$  or  $se(3)$  matrices. Hence, any  $se(3)$ -matrix is given in terms of some twist coordinates.

The Lie bracket on  $se(3)$  is the matrix commutator that assumes the explicit form

$$[\widehat{\mathbf{X}}_1, \widehat{\mathbf{X}}_2] = \widehat{\mathbf{X}}_1 \widehat{\mathbf{X}}_2 - \widehat{\mathbf{X}}_2 \widehat{\mathbf{X}}_1 = \begin{pmatrix} \widehat{\boldsymbol{\xi}}_1 \times \widehat{\boldsymbol{\xi}}_2 & \boldsymbol{\xi}_1 \times \boldsymbol{\eta}_2 - \boldsymbol{\xi}_2 \times \boldsymbol{\eta}_1 \\ \mathbf{0} & 0 \end{pmatrix}. \quad (49)$$

In other words, the Lie bracket of two twists is given by the screw product  $[\mathbf{X}_1, \mathbf{X}_2] = (\boldsymbol{\xi}_1 \times \boldsymbol{\xi}_2, \boldsymbol{\xi}_1 \times \boldsymbol{\eta}_2 - \boldsymbol{\xi}_2 \times \boldsymbol{\eta}_1)$  [62]. This reflects the fact that  $se(3) = so(3) \oplus_s \mathbb{R}^3$  is the semidirect sum of  $so(3)$  and  $\mathbb{R}^3$ . The Lie bracket also embodies the adjoint action of  $se(3)$  on itself, defined as  $\text{ad}_{\widehat{\mathbf{X}}_1} \widehat{\mathbf{X}}_2 = [\widehat{\mathbf{X}}_1, \widehat{\mathbf{X}}_2]$ . Being a linear operator it can be expressed as a matrix acting on screw coordinate vector  $\text{ad}_{\mathbf{X}_1} \mathbf{X}_2$ . For a screw  $\mathbf{X} \in se(3)$  this matrix is

$$\text{ad}_{\mathbf{X}} = \begin{pmatrix} \widehat{\boldsymbol{\xi}} & \mathbf{0} \\ \widehat{\boldsymbol{\eta}} & \widehat{\boldsymbol{\xi}} \end{pmatrix}. \quad (50)$$

This is the matrix representation of the Lie bracket of two twists.

$se(3)$  is isomorphic to the algebra of screws via the identification (48). A screw coordinate vector  $\mathbf{X} = (\boldsymbol{\xi}, \boldsymbol{\eta})$  describes an instantaneous screw motion, i.e. a rotation about the axis  $\boldsymbol{\xi}$  together with a translation along this axis. The latter is given in terms of the position vector  $\mathbf{r}$  of a point on the screw as  $\boldsymbol{\eta} = \mathbf{r} \times \boldsymbol{\xi} + h_{\mathbf{X}} \boldsymbol{\xi}$ , where the scalar  $h_{\mathbf{X}}$  is the pitch of the screw. If  $h_{\mathbf{X}} = 0$ , then  $\mathbf{X}$  are simply the Plücker coordinates of a line along the screw axis. Since any rigid body motion is a finite screw motion it can be expressed in terms of some (time dependent) instantaneous screw coordinates via the exponential mapping.

The exponential mapping, generating  $SE(3)$  from its Lie algebra  $se(3)$ , i.e. the matrix exponential that gives rigid body configuration (46) in terms of screw coordinates, admits the explicit form

$$\mathbf{X} = (\boldsymbol{\xi}, \boldsymbol{\eta}) \mapsto \exp \widehat{\mathbf{X}} = \begin{pmatrix} \exp \widehat{\boldsymbol{\xi}} & \mathbf{dexp}_{\boldsymbol{\xi}} \boldsymbol{\eta} \\ \mathbf{0} & 1 \end{pmatrix} \quad (51)$$

$$= \begin{pmatrix} \exp \widehat{\boldsymbol{\xi}} & \frac{1}{\|\boldsymbol{\xi}\|^2} (\mathbf{I} - \exp \widehat{\boldsymbol{\xi}}) (\boldsymbol{\xi} \times \boldsymbol{\eta}) + h_{\mathbf{X}} \boldsymbol{\xi} \\ \mathbf{0} & 1 \end{pmatrix} \quad (52)$$

with pitch  $h_{\mathbf{X}} := \boldsymbol{\xi} \cdot \boldsymbol{\eta} / \|\boldsymbol{\xi}\|^2$ , and  $\mathbf{dexp}_{\boldsymbol{\xi}}$  from (40). The exponential mapping (51) determines the finite screw motion as a result of the time evolution of the instantaneous screw  $\mathbf{X}(t)$ .

The corresponding twist is determined by the (right) dexp mapping  $\text{dexp} : se(3) \times se(3) \rightarrow se(3)$  as

$$\widehat{\mathbf{V}} = \text{dexp}_{-\widehat{\mathbf{X}}}(\widehat{\dot{\mathbf{X}}}). \quad (53)$$

The expression (39), being applicable to any Lie group, gives rise to several closed forms. A straightforward application of (39) using (50) yields the matrix form [12, 8, 59]

$$\mathbf{dexp}_{\mathbf{X}} = \begin{pmatrix} \mathbf{dexp}_{\boldsymbol{\xi}} & \mathbf{0} \\ \mathbf{P} & \mathbf{dexp}_{\boldsymbol{\xi}} \end{pmatrix} \quad (54)$$

for  $\mathbf{X} = (\boldsymbol{\xi}, \boldsymbol{\eta})$ , where

$$\mathbf{P}(\mathbf{X}) = \frac{\beta}{2} \widehat{\boldsymbol{\eta}} + \frac{1-\alpha}{\|\boldsymbol{\xi}\|^2} (\widehat{\boldsymbol{\eta}} \widehat{\boldsymbol{\xi}} + \widehat{\boldsymbol{\xi}} \widehat{\boldsymbol{\eta}}) + h_{\mathbf{X}} \frac{\alpha - \beta}{\|\boldsymbol{\xi}\|} \widehat{\boldsymbol{\xi}} + \frac{h_{\mathbf{X}}}{\|\boldsymbol{\xi}\|^2} \left( \frac{\beta}{2} - \frac{3(1-\alpha)}{\|\boldsymbol{\xi}\|} \right) \widehat{\boldsymbol{\xi}}^2 \quad (55)$$

with  $\alpha := \frac{2}{\|\boldsymbol{\xi}\|} \sin \frac{\|\boldsymbol{\xi}\|}{2} \cos \frac{\|\boldsymbol{\xi}\|}{2}$ ,  $\beta := \frac{4}{\|\boldsymbol{\xi}\|^2} \sin^2 \frac{\|\boldsymbol{\xi}\|}{2}$ , and the pitch  $h = \boldsymbol{\xi} \cdot \boldsymbol{\eta} / \|\boldsymbol{\xi}\|^2$ . For pure rotation, i.e.  $h_{\mathbf{X}} = 0$ , (55) simplifies. Therewith the vector of the body-fixed twist is given in terms of the time derivative of  $\mathbf{X}$  as  $\mathbf{V} = \mathbf{dexp}_{-\mathbf{X}} \dot{\mathbf{X}}$ .

The inverse of the dexp mapping matrix is readily found as

$$\mathbf{dexp}_{\mathbf{X}}^{-1} = \begin{pmatrix} \mathbf{dexp}_{\boldsymbol{\xi}}^{-1} & \mathbf{0} \\ \mathbf{U} & \mathbf{dexp}_{\boldsymbol{\xi}}^{-1} \end{pmatrix} \quad (56)$$

with

$$\mathbf{U}(\mathbf{X}) = \frac{1-\gamma}{\|\boldsymbol{\xi}\|^2} (\widehat{\boldsymbol{\eta}} \widehat{\boldsymbol{\xi}} + \widehat{\boldsymbol{\xi}} \widehat{\boldsymbol{\eta}}) + \frac{h_{\mathbf{X}}}{\|\boldsymbol{\xi}\|^3} \left( \frac{1}{\beta} + \gamma - 2 \right) \widehat{\boldsymbol{\xi}}^2 - \frac{1}{2} \widehat{\boldsymbol{\eta}} \quad (57)$$

and  $\gamma := \frac{2}{\|\boldsymbol{\xi}\|} \cot \frac{\|\boldsymbol{\xi}\|}{2}$ . Another closed form expression was reported in [62]

$$\mathbf{dexp}_{\mathbf{X}}^{-1} = \mathbf{I} - \frac{1}{2} \mathbf{ad}_{\mathbf{X}} + \left( \frac{2}{\|\boldsymbol{\xi}\|^2} + \frac{\|\boldsymbol{\xi}\| + 3 \sin \|\boldsymbol{\xi}\|}{4 \|\boldsymbol{\xi}\| (\cos \|\boldsymbol{\xi}\| - 1)} \right) \mathbf{ad}_{\mathbf{X}}^2 + \left( \frac{1}{\|\boldsymbol{\xi}\|^4} + \frac{\|\boldsymbol{\xi}\| + \sin \|\boldsymbol{\xi}\|}{4 \|\boldsymbol{\xi}\|^3 (\cos \|\boldsymbol{\xi}\| - 1)} \right) \mathbf{ad}_{\mathbf{X}}^4. \quad (58)$$

The formulations (54) and (58) admit reformulating the kinematic relation as explicit ODE  $\dot{\mathbf{X}} = \mathbf{dexp}_{-\mathbf{X}}^{-1} \mathbf{V}$ .

**Remark 4.** *It is instructive to show how the 3-parameter description of rotations fits into the Lie group formulation. If rotations are described by successive rotations about intermediate axes the rotation matrix is given as  $\mathbf{R} = \exp(\widehat{\mathbf{e}}_i \theta_i) \exp(\widehat{\mathbf{e}}_j \theta_j) \exp(\widehat{\mathbf{e}}_k \theta_k)$ , where  $\mathbf{e}_i, \mathbf{e}_j, \mathbf{e}_k$  are constant unit vectors along the intermediate instantaneous rotation axes, and  $\theta_i, \theta_j, \theta_k$  are the corresponding rotation angles. The only condition is  $\mathbf{e}_i \neq \mathbf{e}_j, \mathbf{e}_j \neq \mathbf{e}_k$ . In particular, using  $i = k = 3, j = 1$  corresponds to the Euler angle description, which is called 'degenerate' since  $\mathbf{e}_i = \mathbf{e}_k$ . Setting  $i = 1, j = 2, k = 3$  yields the Bryant/Cardan angle parameterization. Noting that for constant  $\mathbf{e}_i$  in  $\mathbf{R}_i = \exp(\widehat{\mathbf{e}}_i \theta_i)$ ,  $\mathbf{R}_i^{-1} \dot{\mathbf{R}}_i = \mathbf{dexp}_{\mathbf{e}_i \theta_i}(\widehat{\mathbf{e}}_i \dot{\theta}_i) = \widehat{\mathbf{e}}_i \dot{\theta}_i$ , etc., the corresponding angular velocity is*

$$\boldsymbol{\omega} = \begin{pmatrix} \mathbf{R}_k^T \mathbf{R}_j^T \mathbf{e}_i & \mathbf{R}_k^T \mathbf{e}_j & \mathbf{e}_k \end{pmatrix} \begin{pmatrix} \dot{\theta}_i \\ \dot{\theta}_j \\ \dot{\theta}_k \end{pmatrix} = \mathbf{B} \dot{\boldsymbol{\theta}} \quad (59)$$

as in (2). E.g. for  $i = k = 3, j = 1$ , these are the kinematic Euler equations, and the  $3 \times 3$  matrix in (59) is the corresponding coefficient matrix [45]. This is easily extended to  $SE(3)$  by using a unit basis including translations.

### A.3 Direct Product Representation of Rigid Body Configurations and Mixed Velocity Representation

If the concatenation of frame transformations is ignored, a rigid body configuration can simply be regarded as  $C = (\mathbf{R}, \mathbf{r}) \in SO(3) \times \mathbb{R}^3$ . That is, the configuration space of a rigid body is the direct product of  $SO(3)$  and  $\mathbb{R}^3$  with group multiplication

$$C_1 \cdot C_2 = (\mathbf{R}_1 \mathbf{R}_2, \mathbf{r}_1 + \mathbf{r}_2). \quad (60)$$

This does clearly not represent a frame transformation, i.e. a rigid body motion. Nevertheless it is commonly used as geometric model for MBS kinematics giving rise to the equations (2), and for Lie group integration

methods of rigid body dynamics [19, 21, 26, 39, 68]. The drawback becomes critical if the multiplication (60) is employed in the position update of integration schemes as will be shown later.

The inverse element is  $(\mathbf{R}, \mathbf{r})^{-1} = (\mathbf{R}^T, -\mathbf{r})$ . If desired,  $SO(3) \times \mathbb{R}^3$  can be represented by the group of  $7 \times 7$  matrices of the form

$$\mathbf{C} = \begin{pmatrix} \mathbf{R} & \mathbf{0} & \mathbf{0} \\ \mathbf{0} & \mathbf{I} & \mathbf{r} \\ \mathbf{0} & \mathbf{0} & 1 \end{pmatrix}, \text{ with } \mathbf{R} \in SO(3), \mathbf{r} \in \mathbb{R}^3. \quad (61)$$

The product (60) is then represented by  $\mathbf{C}_1 \cdot \mathbf{C}_2$ . The Lie algebra of the direct product  $SO(3) \times \mathbb{R}^3$  is the direct sum  $so(3) \oplus \mathbb{R}^3$  whose elements can also be represented as vectors  $\mathbf{X} = (\boldsymbol{\xi}, \mathbf{r}) \in \mathbb{R}^6$ . With  $\mathbb{R}^3$  being a commutative algebra, the Lie bracket on this algebra is

$$[\mathbf{X}_1, \mathbf{X}_2] = (\boldsymbol{\xi}_1 \times \boldsymbol{\xi}_2, \mathbf{0}). \quad (62)$$

This can be expressed as  $\mathbf{ad}_{\mathbf{X}_2} \mathbf{X}_1$  with matrix

$$\mathbf{ad}_{\mathbf{X}} = \begin{pmatrix} \hat{\boldsymbol{\xi}} & \mathbf{0} \\ \mathbf{0} & \mathbf{0} \end{pmatrix}. \quad (63)$$

If the matrix representation (61) is used, the corresponding Lie algebra consists of matrices

$$\hat{\mathbf{X}} = \begin{pmatrix} \hat{\boldsymbol{\xi}} & \mathbf{0} & \mathbf{0} \\ \mathbf{0} & \mathbf{0} & \mathbf{r} \\ \mathbf{0} & \mathbf{0} & 0 \end{pmatrix}, \text{ with } \hat{\boldsymbol{\xi}} \in so(3), \mathbf{r} \in \mathbb{R}^3 \quad (64)$$

with matrix commutator as Lie bracket. The exponential mapping on the direct product group is

$$\mathbf{X} = (\boldsymbol{\xi}, \mathbf{r}) \longmapsto \exp \mathbf{X} = (\exp \hat{\boldsymbol{\xi}}, \mathbf{r}) \quad (65)$$

with the exponential mapping (38) on  $SO(3)$ . Apparently  $\mathbf{X}$  is not a screw coordinate vector, but rather consists of a rotation and a translation vector. The exponential of (64) yields the matrices (61).

The rigid body velocity for  $C(t) = (\mathbf{R}, \mathbf{r}) \in SO(3) \times \mathbb{R}^3$  is introduced in vector notation as  $\mathbf{V}^m = (\boldsymbol{\omega}, \mathbf{v}^s)$  with  $\mathbf{v}^s := \dot{\mathbf{r}}$ . This is not a proper twist. It contains an apparent mix of body-fixed angular velocity  $\boldsymbol{\omega}$  and spatial linear velocity  $\mathbf{v}^s \equiv \dot{\mathbf{r}}$ , and is therefore commonly referred to as *mixed representation* of rigid body velocities. With (64) this is, in analogy to (48), defined by

$$\hat{\mathbf{V}}^m := \mathbf{C}^{-1} \dot{\mathbf{C}} \quad \text{with} \quad \hat{\mathbf{V}}^m = \begin{pmatrix} \hat{\boldsymbol{\omega}} & \mathbf{0} & \mathbf{0} \\ \mathbf{0} & \mathbf{0} & \mathbf{v}^s \\ \mathbf{0} & \mathbf{0} & 0 \end{pmatrix} \in so(3) \times \mathbb{R}^3. \quad (66)$$

The dexm mapping corresponding to (65) is

$$\text{dexm}_{\mathbf{X}_1}(\mathbf{X}_2) = (\text{dexm}_{\hat{\boldsymbol{\xi}}_1}(\hat{\boldsymbol{\xi}}_2), \mathbf{r}_2) \quad (67)$$

with the dexm mapping on  $SO(3)$  in (40). In vector form of the mixed velocity, the relation

$$\mathbf{V}^m = \text{dexm}_{-\mathbf{X}} \dot{\mathbf{X}} = \begin{pmatrix} \text{dexm}_{-\hat{\boldsymbol{\xi}}} & \mathbf{0} \\ \mathbf{0} & \mathbf{I} \end{pmatrix} \begin{pmatrix} \dot{\boldsymbol{\xi}} \\ \dot{\mathbf{r}} \end{pmatrix} \quad (68)$$

for  $\mathbf{X} = (\boldsymbol{\xi}, \mathbf{r})$ , resembles (2). In fact the angular and linear velocities are considered as decoupled. The matrix  $\text{dexm}_{-\hat{\boldsymbol{\xi}}}$  in (68) is the matrix  $\mathbf{B}$  in (2) when the rotation vector parameterization is used. Moreover, (68) covers any general 3-angle parameterization by concatenation of three successive mappings as in (59).

**Remark 5.** In applications frequently the mixed velocity  $\mathbf{V}^m = (\boldsymbol{\omega}, \dot{\mathbf{r}})$  is used (section A.3). If desired, the body-fixed twist can be transformed to the mixed velocity. Since  $\dot{\mathbf{r}} = \mathbf{R}\mathbf{v}$  this is achieved by premultiplication of the second column in (54) with  $\mathbf{R} = \exp \hat{\boldsymbol{\xi}}$ . Noting that  $\exp \hat{\boldsymbol{\xi}} \cdot \mathbf{dexp}_{-\hat{\boldsymbol{\xi}}} = \mathbf{dexp}_{\hat{\boldsymbol{\xi}}}$  this leads to the expression  $\mathbf{V}^m = \mathbf{A}(\mathbf{X}) \dot{\mathbf{X}}$  with

$$\mathbf{A}(\mathbf{X}) := \begin{pmatrix} \mathbf{I} & \mathbf{0} \\ \mathbf{0} & \mathbf{R} \end{pmatrix} \cdot \mathbf{dexp}_{-\mathbf{X}} = \begin{pmatrix} \mathbf{dexp}_{-\boldsymbol{\xi}} & \mathbf{0} \\ \mathbf{R} \cdot \mathbf{P}(-\mathbf{X}) & \mathbf{dexp}_{\boldsymbol{\xi}} \end{pmatrix}. \quad (69)$$

**Remark 6.** The matrix representation (66) is not used in implementations but merely introduced to emphasize the formally identical definition of velocity (48) and (66) for both groups, used in the general form of the motion equations in section 3.3. The kinematic reconstruction equations (3) are generally valid and only the c-space Lie group is to be replaced. The velocities are left-invariant vector fields. For  $SE(3)$  this means that they are invariant w.r.t. changes of global reference frame (described by left multiplication of  $C$ ).

In summary the only difference of the two c-space representations is the concatenation of configurations, but this is the critical aspect for numerical reconstruction of finite motions from velocities where the solution is advanced from one time step to the next by an incremental motion. In other words, both,  $SE(3)$  and  $SO(3) \times \mathbb{R}^3$ , can be used to represent the *configuration* of a rigid body but only  $SE(3)$  allows for representing rigid body *motions*. In particular successive frame transformations, i.e. concatenation of successive configurations, (47) and (60), respectively, reveal the fundamental difference, which is accordingly reflected in the exp mapping.

#### A.4 Proper Rigid Body Motions in Terms of Dual Quaternions

The fact that there is no 3-parametric global parameterization of rotations leads to the well-known problem of parameterization singularities on  $SO(3)$  and any product group. This is apparent from the axis-angle description, i.e. using exponential coordinates  $\boldsymbol{\xi}$ , since (40), respectively (54), is singular for  $\|\boldsymbol{\xi}\| = \pm k\pi, k \in \mathbb{N}$ . This can only be avoided by using redundant parameters like Euler parameters (instead of three independent in  $\boldsymbol{\xi}$ ), or by avoiding the introduction of local coordinates at all (see appendix B). The use of dependent global coordinates corresponds to replace  $SE(3)$  and  $SO(3) \times \mathbb{R}^3$  by their covering Lie groups. This is outlined in the this and next section.

The rigid body motion group  $SE(3)$  is homomorphic to the group of dual quaternions,  $\mathbb{H}_\varepsilon$  [44, 70]. An ordinary quaternion is written as 4-vector  $\mathbf{Q} = (q_0, \mathbf{q}) \in \mathbb{H}$  where the vector part is  $\mathbf{q} = (q_1, q_2, q_3)$ . Euler parameters are unit quaternions, i.e.  $\|\mathbf{Q}\| = 1$ , used to parameterize spatial rotations. Dual quaternions are generalizations of ordinary quaternions. Avoiding using dual numbers, a dual quaternion can be expressed as an 8-dimensional vector  $\hat{\mathbf{Q}} = (\mathbf{Q}, \mathbf{Q}_\varepsilon)$ , where  $\mathbf{Q} \in \mathbb{H}$  is a unit quaternion and  $\mathbf{Q}_\varepsilon$  is another quaternion satisfying the Plücker condition  $\mathbf{Q} \cdot \mathbf{Q}_\varepsilon = 0$ . The Euler parameters  $\mathbf{Q}$  describe the rotation and  $\mathbf{Q}_\varepsilon$  the translation of a frame transformation. That is, a frame transformation  $C = (\mathbf{R}, \mathbf{r}) \in SE(3)$ , and thus its screw coordinates  $\mathbf{X} = (\boldsymbol{\xi}, \boldsymbol{\eta})$ , can be mapped to a dual quaternion. This is called the kinematic image space transformation or kinematic mapping [6, 14, 61, 66].

Multiplication of dual quaternions is expressible in matrix form as [29]

$$\hat{\mathbf{Q}}\hat{\mathbf{P}} = \hat{\mathbf{Q}}^+\hat{\mathbf{P}} = \hat{\mathbf{P}}^-\hat{\mathbf{Q}} \quad (70)$$

with

$$\hat{\mathbf{Q}}^+ = \begin{pmatrix} \mathbf{Q}^+ & \mathbf{0} \\ \mathbf{Q}_\varepsilon^+ & \mathbf{Q}^+ \end{pmatrix}, \quad \hat{\mathbf{Q}}^- = \begin{pmatrix} \mathbf{Q}^- & \mathbf{0} \\ \mathbf{Q}_\varepsilon^- & \mathbf{Q}^- \end{pmatrix} \quad (71)$$

and the Hamilton matrices

$$\mathbf{Q}^+ = \begin{pmatrix} q_0 & -\mathbf{q}^T \\ \mathbf{q} & q_0\mathbf{I}_3 + \hat{\mathbf{q}} \end{pmatrix}, \quad \mathbf{Q}^- = \begin{pmatrix} q_0 & -\mathbf{q}^T \\ \mathbf{q} & q_0\mathbf{I}_3 - \hat{\mathbf{q}} \end{pmatrix}. \quad (72)$$

The rotation matrix corresponding to  $\mathbf{Q}$  is given as  $\mathbf{R} = \mathbf{D}\mathbf{E}^T$  with

$$\mathbf{D}(\mathbf{Q}) = \begin{pmatrix} -\mathbf{q} & q_0\mathbf{I}_3 + \hat{\mathbf{q}} \end{pmatrix}, \quad \mathbf{E}(\mathbf{Q}) = \begin{pmatrix} -\mathbf{q} & q_0\mathbf{I}_3 - \hat{\mathbf{q}} \end{pmatrix}. \quad (73)$$

The corresponding Cartesian position vector  $\mathbf{r}$  is given by the vector part of

$$\begin{pmatrix} 0 \\ \mathbf{r} \end{pmatrix} = 2\mathbf{Q}^{-T}\mathbf{Q}_\varepsilon. \quad (74)$$

The mixed velocity  $\mathbf{V}^m = (\boldsymbol{\omega}, \mathbf{v}^s)$  is then given as

$$\mathbf{V}^m = \mathbf{H}^m(\hat{\mathbf{Q}})\dot{\hat{\mathbf{Q}}} \quad (75)$$

with

$$\mathbf{H}^m(\hat{\mathbf{Q}}) := 2 \begin{pmatrix} \mathbf{D}(\mathbf{Q}) & \mathbf{0} \\ -\mathbf{D}(\mathbf{Q}_\varepsilon) & \mathbf{D}(\mathbf{Q}) \end{pmatrix}. \quad (76)$$

Using  $\mathbf{v} = \mathbf{E}\mathbf{D}^T\mathbf{v}^s$  and  $\mathbf{E}\mathbf{D}^T\mathbf{D} = \|\mathbf{Q}\|\mathbf{E}$  with  $\|\mathbf{Q}\| = 1$ , the body-fixed twist is

$$\mathbf{V} = \mathbf{H}(\hat{\mathbf{Q}})\dot{\hat{\mathbf{Q}}} \quad (77)$$

with

$$\mathbf{H}(\hat{\mathbf{Q}}) := \begin{pmatrix} \mathbf{D}(\mathbf{Q}) & \mathbf{0} \\ -\mathbf{E}(\mathbf{Q})\mathbf{D}^T(\mathbf{Q})\mathbf{D}(\mathbf{Q}_\varepsilon) & \mathbf{E}(\mathbf{Q}) \end{pmatrix}. \quad (78)$$

In summary, a frame transformation (a proper rigid body motion) is represented by a dual quaternion, and the screw coordinates  $\mathbf{X} = (\boldsymbol{\xi}, \boldsymbol{\eta}) \in \mathbb{R}^6$  are replaced by the dual quaternion  $\mathbf{X} = (\mathbf{Q}, \mathbf{Q}_\varepsilon) \in \mathbb{H}_\varepsilon$  that serve as dependent global coordinates. The two  $(\mathbf{Q}, \mathbf{Q}_\varepsilon)$  and  $(\mathbf{Q}^*, \mathbf{Q}_\varepsilon)$  correspond to the same frame transformation  $C \in SE(3)$ , where  $\mathbf{Q}^*$  is the conjugate of  $\mathbf{Q}$ . Relation (77) and (75) is the counterpart of (54) and (69), respectively.

**Remark 7.** *It may seem unnecessary to replace both, the parameterization of rotation and translation by quaternions. But this is indeed necessary in order to retain the semidirect product structure of  $SE(3)$ , i.e. the coupling of rotation and translation. This is apparent from (54) since even if the upper left dexp mapping is replaced by  $\mathbf{D}$  the one in the lower right corner cannot be replaced.*

#### A.5 Direct Product Representation in Terms of Euler Parameters

The substitution of the rotation parameters in the direct product group is straightforward.  $SO(3) \times \mathbb{R}^3$  is homomorphic to  $\mathbb{H} \times \mathbb{R}^3$ , and Euler parameters can be introduced immediately as global coordinates on  $SO(3)$ . Denote  $\mathbf{X} = (\mathbf{Q}, \mathbf{r}) \in \mathbb{H} \times \mathbb{R}^3$ , then

$$\mathbf{V}^m = \mathbf{H}^m(\mathbf{X})\dot{\mathbf{X}} \quad (79)$$

with

$$\mathbf{H}^m(\mathbf{Q}, \mathbf{r}) := 2 \begin{pmatrix} \mathbf{D}(\mathbf{Q}) & \mathbf{0} \\ \mathbf{0} & \mathbf{I}_3 \end{pmatrix} \quad (80)$$

replacing (68). The direct product  $SO(3) \times \mathbb{R}^3$  is thus replaced by the direct product  $\mathbb{H} \times \mathbb{R}^3$ .

## B Munthe-Kaas Integration Method for Kinematic Reconstruction on C-Space Lie Groups using Local Coordinates

The vector space ODEs (14) and (15) can be solved with any established numerical integration scheme. Integration of (17) requires application of Lie group integration schemes. Several numerical schemes were developed for solving system of the form (17b). Munthe-Kaas (MK) and Crouch-Grossman methods are the best-known [38, 27]. The basic idea behind the MK integration scheme is to replace the equation (17b) on  $G$  by a vector space ODE on  $\mathfrak{g}$  and to solve this by a standard vector space integration method. The MK method was originally introduced for right translated equations, i.e. of the form  $\dot{g} = \widehat{\mathbf{V}}g$  [43, 50, 51, 52, 55]. It is adapted to the left translated form (17b) in the following. Starting from an initial value  $g_0 \in G$  a solution of (17b) can be expressed in the form  $g(t) = g_0 \exp \widehat{\Phi}(t)$ , with  $\Phi(0) = 0$ , where  $\Phi(t)$  is a curve in  $\mathfrak{g}$ . It is known that  $\Phi$  must satisfy the linear ODE

$$\dot{\Phi}(t) = \text{dexp}_{-\Phi(t)}^{-1} \mathbf{V}(t, g(t)), \text{ with } \Phi(0) = 0 \quad (81)$$

which is commonly attributed to Hausdorff [36, 41]. Hence, although it is not involved in the formulation of the reconstruction equations (17b), the  $\text{dexp}$  mapping appears again in the integration scheme. In the MK method (81) is solved with an explicit Runge-Kutta (RK) method.

At the integration step  $i$ , i.e. in the transition from time  $t_{i-1}$  to  $t_i$ , the system

$$\dot{\Phi} = \text{dexp}_{-\Phi}^{-1} \mathbf{V}(t, g_{i-1} \exp \Phi), \quad t \in [t_{i-1}, t_i], \text{ with } \Phi(t_{i-1}) = 0 \quad (82)$$

is solved with a RK scheme to obtain a solution  $\Phi^{(i)} := \Phi(t_i)$ . The numerical solution of (17b) is then advanced as  $g_i := g_{i-1} \exp \Phi^{(i)}$ .  $g_0$  is the initial configuration of the MBS (satisfying the assembly constraints). Resorting to the RK method an explicit  $s$ -stage MK scheme at time step  $i$  with step size  $\Delta t$  follows immediately as

$$\begin{aligned} g_i &:= g_{i-1} \exp \widehat{\Phi}^{(i)} \\ \Phi^{(i)} &:= \Delta t \sum_{j=1}^s b_j \mathbf{k}_j \\ \mathbf{k}_j &:= \text{dexp}_{-\Psi_j}^{-1} \mathbf{V}(t_{i-1} + c_j \Delta t, g_{i-1} \exp \widehat{\Psi}_j) \\ \Psi_j &:= \Delta t \sum_{l=1}^{j-1} a_{jl} \mathbf{k}_l, \quad \Psi_1 = 0 \end{aligned} \quad (83)$$

where  $a_{jl}$ ,  $b_j$ , and  $c_j$  are the Butcher coefficients of the  $s$ -stage RK method, and  $\mathbf{k}_j, \Psi_j \in \mathfrak{g}$ .

The equations (17b) are indeed not independent and dynamics simulation requires integrating the dynamics equations (17a) with the same RK scheme, so that the overall system (17) is integrated with one RK scheme. Moreover, since the MK method reduces to the vector space RK scheme, the motion equations (17) can be treated as a system on a state space Lie group and integrated with the MK method. This will be reported in a forthcoming publication giving special attention to constraint stabilization. Furthermore, an appropriate integration method can be used to integrate (17) according to their numerical conditioning, and the RK method be replaced accordingly in the MK scheme.

**Remark 8.** *Although the ODE (17) is coordinate-free the  $\Phi^{(i)}$  serve as local coordinates on the  $c$ -space. Thus a coordinate patch on  $G$  is defined during the integration. This parameterization can be assumed singularity-free since each  $\Phi^{(i)}$  need only cover a finite neighborhood of  $g_{i-1}$ , depending on the step size and the actual dynamics.*

**Remark 9.** *Notice that integration of the motion equations (12) with a RK method is equivalent to the MK scheme (83) where global exponential coordinates  $\mathbf{q}$  are used, instead of local coordinates  $\Phi$ , and the configuration update is  $g_i := g_0 \exp \mathbf{q}^{(i)}$ . This underlines again that the Lie group concept is just another way of looking at the rigid body kinematics.*

## REFERENCES

- 1 J. Angeles: Fundamentals of robotic mechanical systems - second edition, Springer, 2003
- 2 O.A. Bauchau, A. Laulusa, *Review of contemporary approaches for constraint enforcement in multibody systems*, J. Comput. Nonlinear Dynam. Vol. 3, 2008

- 3 J. Baumgarte: *Stabilization of constraints and integrals of motion in dynamical systems*, Computer Methods in Applied Mechanics and Engineering, Vol. 1, 1972, pp. 1-16
- 4 E. Bayo, R. Ledesma: *Augmented lagrangian and mass-orthogonal projection methods for constrained multi-body dynamics*, Nonlinear Dynamics, Vol. 9, No. 1-2, 1996, pp. 113-130
- 5 W. Blajer: *Methods for constraint violation suppression in the numerical simulation of constrained multibody systems – A comparative study*, Comput. Methods Appl. Mech. Engrg. Vol. 200, 2011, pp. 1568–1576
- 6 W. Blaschke: *Nicht-Euklidische Geometrie und Mechanik, Vol. I, II, III*, Teubner, Leipzig, 1942
- 7 M. Borri, C.L. Bottasso: An intrinsic beam model based on a helicoidal approximation - Part I: Formulation International Journal of Numerical Methods in Engineering, 37, 1994, pp. 2267-2289
- 8 M. Borri, C.L. Bottasso, L. Trainelli: Integration of Elastic Multibody Systems by Invariant Conserving/Dissipating Algorithms - Part I : Formulation Computer Methods in Applied Mechanics and Engineering, Vol. 190 (29/30), 2001, pp. 3669-3699
- 9 M. Borri, C.L. Bottasso, L. Trainelli: Integration of Elastic Multibody Systems by Invariant Conserving/Dissipating Algorithms - Part II : Numerical Schemes and Applications Computer Methods in Applied Mechanics and Engineering, Vol. 190 (29/30), 2001, pp. 3701-3733
- 10 M. Borri, C.L. Bottasso, L. Trainelli: A Novel Momentum-Preserving/Energy-Decaying Algorithm for Finite-Element Multibody Procedures Computer Assisted Mechanics and Engineering Sciences, Vol. 9 (3), 2002, pp. 315-340
- 11 M. Borri, C.L. Bottasso, L. Trainelli: An Invariant-Preserving Approach to Robust Finite-Element Multibody Simulation Zeitschrift für Angewandte Mathematik und Mechanik, Vol. 83 (10), 2003, pp. 663-676
- 12 C.L. Bottasso, M. Borri: Integrating finite rotations, Comput. Methods Appl. Mech. Engrg., Vol. 164, 1998, pp. 307-331
- 13 C.L. Bottasso, M. Borri, L. Trainelli: Geometric Invariance, Computational Mechanics, Vol. 29 (2), 2002, pp. 163-169
- 14 O. Bottema, B. Roth: Theoretical Kinematics, North Holland Publ. Amsterdam, 1979
- 15 H. Brauchli: Mass-orthogonal formulation of equations of motion for multibody systems, Zeitschrift für Angewandte Mathematik und Physik (ZAMP), Vol. 42, No. 2, 1991, pp. 169-182
- 16 D.J. Braun, M. Goldfarb: Eliminating constraint drift in the numerical simulation of constrained dynamical systems, Computer Methods in Applied Mechanics and Engineering, Vol. 198, No. 37-40, 2009, pp. 3151-3160
- 17 R. W. Brockett: Robotic manipulators and the product of exponentials formula, Mathematical Theory of Networks and Systems, Lecture Notes in Control and Information Sciences Vol. 58, 1984, pp 120-129
- 18 V. Brodsky, M. Shoam: *Dual numbers representation of rigid body dynamics*, Mech. Mach. Theory, Vol. 34, No. 5, 1999, pp. 693-718
- 19 O. Brüls, A. Cardona: *On the Use of Lie Group Time Integrators in Multibody Dynamics*, J. Comput. Nonlinear Dynam., Vol. 5, No 3, 2010
- 20 O. Brüls, A. Cardona, M. Arnold: *Two lie group formulations for dynamic multibody systems with large rotations*, Proc ASME Int. Design Eng. Tech. Conf. IDETC 2011, August 28-31, 2011, Washington, USA
- 21 O. Brüls, A. Cardona, M. Arnold: *Lie group generalized-alpha time integration of constrained flexible multibody systems*, Mech. Mach. Theory, Vol. 48, 2012, pp. 121-137
- 22 F. Bullo, R.M. Murray: *Proportional Derivative (PD) Control on the Euclidean group*, CDS technical report 95-010, 1995
- 23 D.P. Chevallier: La formation des équations de la dynamique. Examen des diverses méthodes, Mécanique, 1984
- 24 D.P. Chevallier: Lie Groups and Multibody Dynamics Formalism, Proc. EUROMECH Colloquium 320, Prague, 1994, pp. 1-20
- 25 R. Chhabra, M.R. Emami: A generalized exponential formula for forward and differential kinematics of open-chain multi-body systems, Mechanism and Machine Theory, 2014, Vol. 73, pp. 61-75
- 26 E. Celledoni, B. Owren: *Lie Group Methods for Rigid Body Dynamics and Time Integration on Manifolds*, Computer Methods in Applied Mechanics and Engineering, Vol. 19, 1999, pp. 421-438
- 27 P. E. Crouch, R. Grossman, Numerical integration of ordinary differential equations on manifolds, J. Nonlinear Sci., Vol. 3, No. 1, 1993, pp. 1-33
- 28 F.M. Dimentberg: *The Screw Calculus and Its Applications in Mechanics*, Foreign Technology Division translation, Wright-Patterson AFB, Ohio, FTD-HT-1632-67, 1965
- 29 J.R. Dooley, J.M. McCarthy: Spatial Rigid Body Dynamics using Dual Quaternions, Proc. IEEE Int. Conf. Rob. Automat (ICRA), 1991, pp. 90-95
- 30 S. Erlicher, L. Bonaventura, O. Bursi: The analysis of the generalized-alpha method for non-linear dynamic problems. Computational Mechanics Vol. 28, 2002, pp. 83-104
- 31 K. Engø, A. Marthinsen: *A Note on the Numerical Solution of the Heavy Top Equations*, Multibody System Dynamics Vol. 5, 2001, pp. 387-397

- 32 R. Featherstone: *Rigid Body Dynamics Algorithms*, Springer, 2008
- 33 J. Garcia de Jalon, E. Bayo: *Kinematic and Dynamic Simulation of Multibody Systems. The Real Time Challenge*. Springer-Verlag, 1994
- 34 C.G. Gibson, K.H. Hunt: Geometry of screw systems - 1: Screws: Genesis and geometry, *Mech. Mach. Theory*, Vol. 25, No. 1, 1990, pp. 1-10
- 35 C.G. Gibson, K.H. Hunt: Geometry of screw systems - 2: classification of screw systems, *Mech. Mach. Theory*, Vol. 25, No. 1, 1990, pp. 11-27
- 36 E. Hairer, C. Lubich, G. Wanner: *Geometric Numerical Integration*, Springer, 2006
- 37 K.H. Hunt: *Kinematic geometry of mechanisms*, Clarendon Press, 1978
- 38 A. Iserles, H.Z. Munthe-Kaas, S.P. Nørsett, A. Zanna: Lie-group methods, *Acta Numerica* (2000), pp. 215-365
- 39 P. Krysl, L. Endres: Explicit Newmark/Verlet algorithm for time integration of the rotational dynamics of rigid bodies, *Int. J. Numer. Meth. Engng.* Vol. 62, 2005, pp. 2154-2177
- 40 Y. Liu: Screw-matrix method in dynamics of multibody systems, *Acta Mechanica Sinica*, Vol. 4, No. 2, 1988, pp. 165-174
- 41 W. Magnus: On the exponential solution of differential equations for a linear operator, *Comm. Pure Appl. Math.* VII, 1954, pp. 649-673
- 42 J. Mäkinen: Critical Study of Newmark-scheme on manifold of finite rotations, *Comp. Methods Appl. Engrg.*, Vol. 191, 2001, pp. 817-828
- 43 A. Marthinsen, H. Munthe-Kaas, B. Owren: *Simulation of Ordinary Differential Equations on Manifolds - Some Numerical Experiments and Verifications*, *Modeling, Identification and Control*, Vol. 18, No. 1, 1997, pp. 75-88
- 44 M.C. McCarthy, G.S. Soh: *Geometric Design of Linkages*, Springer, 2nd ed. 2011
- 45 J.L. McCauley: *Classical Mechanics*, Cambridge University Press, 1997
- 46 C. Mladenova: Applications of Lie Group Theory to the Modeling and Control of Multibody Systems, *Multibody System Dynamics*, Vol. 3, No. 4, 1999, pp. 367-380
- 47 C.D. Mladenova: Group Theory in the Problems of Modeling and Control of Multi-Body Systems, *Journal of Geometry and Symmetry in Physics*, Vol. 8, 2006, pp. 17-121
- 48 A. Müller, P. Maisser: *Lie group formulation of kinematics and dynamics of constrained MBS and its application to analytical mechanics*, *Multibody Syst. Dynam.*, Vol. 9, 2003, pp. 311-352
- 49 A. Müller, Z. Terze: *Is there an optimal choice of configuration space for Lie group integration schemes applied to constrained MBS?*, *Proc ASME Int. Design Eng. Tech. Conf. IDETC 2013*, August 12-15, 2013, Portland, USA
- 50 H. Munthe-Kaas, *Runge Kutta methods on Lie groups*, *BIT*, Vol. 38, No. 1, 1998, pp. 92-111
- 51 H. Munthe-Kaas, *High order Runge-Kutta methods on manifolds*, *Appl. Numer. Math.*, Vol. 29, 1999, pp. 115-127
- 52 H. Munthe-Kaas, B. Owren: *Computations in a free Lie algebra*, *Phil. Trans. Royal Soc. A*, 357: 957-981, 1999
- 53 R.M Murray, Z. Li, S. S. Sastry: *A mathematical Introduction to robotic Manipulation*, CRC Press, 1993
- 54 N.M. Newmark: A Method of Computation for Structural Dynamics, *J. Engineering Mechanics Division ASCE*, Vol. 85, No. EM3, 1959, pp. 67-94
- 55 B. Owren, A. Marthinsen: Runge-Kutta methods adapted to manifolds and based in rigid frames, *BIT*, Vol. 39, 1999, pp. 116-142
- 56 F. C. Park, J. E. Bobrow, S. R. Ploen: A Lie group formulation of robot dynamics, *Int. J. Rob. Research*, Vol. 14, No. 6, 1995, pp. 609-618
- 57 F.C. Park: Computational Aspects of the Product-of-Exponentials Formula for Robot Kinematics, *IEEE Trans. Aut. Contr.* Vol. 39, No. 3, 1994, 643-647
- 58 F.C. Park, M.W. Kim: Lie theory, Riemannian geometry, and the dynamics of coupled rigid bodies, *Z. angew. Math. Phys.*, Vol. 51, 2000, pp. 820-834
- 59 J. Park, W.K. Chung: Geometric integration on Euclidean group with application to articulated multibody systems, *IEEE Trans. Rob. Automat.* Vol. 21, No. 5, 2005, pp. 850-863
- 60 S.R. Ploen, F.C. Park: A Lie group formulation of the dynamics of cooperating robot systems, *Rob. and Auton. Sys.*, Vol. 21, 1997, pp. 279-287
- 61 B. Ravani, B. Roth: Mappings of Spatial Kinematics, *J. Mech. Des.* Vol. 106. No. 3, 1984, pp. 341-347
- 62 J.M. Selig: *Geometrical Methods in Robotics*, Springer, New York, 1996.
- 63 J.M. Selig: Cayley Maps for SE(3), 12th IFToMM World Congress, Beacon, June 18-21, 2007
- 64 B. Siciliano, O. Khatib: *Springer Handbook of Robotics*, Springer-Verlag Berlin Heidelberg, 2008
- 65 J.C. Simo: *A finite strain beam formulation. The three-dimensional dynamic problem. Part 1*, *Computer Methods in Applied Mechanics and Engineering*, Vol. 49, No. 1, 1985, pp. 55-70



- 66 E. Study, *Von den Bewegungen und Umlegungen*, Math. Ann., 39, 1891, pp. 441–566
- 67 Z. Terze, J. Naudet: *Geometric properties of projective constraint violation stabilization method for generally constrained multibody systems on manifolds*, Multibody Syst. Dynam. Vol. 20, 2008, pp. 85-106
- 68 Z. Terze, A. Müller, D. Zlatar: *DAE Index 1 Formulation for Multibody System Dynamics in Lie-Group Setting*, 2nd Joint Int. Conf. on Multibody System Dynamics (IMSD), May 29-June 1, 2012, Stuttgart, Germany
- 69 J.J. Uicker, B. Ravani, P.N. Sheth: *Matrix Methods in the Design Analysis of Mechanisms and Multibody Systems*, Cambridge University Press, 2013
- 70 A. T. Yang, F. Freudenstein: *Application of Dual-Number Quaternion Algebra to the Analysis of Spatial Mechanisms*, J. Appl. Mech., Vol. 31(2), 1964, pp. 300-308

$\omega$  $\xi$  $\omega_0$  $\mathbf{p}_i$  $\mathbf{p}_{i+1/2}$  $\mathbf{v}_i$  $\mathbf{v}_{i+1/2}$  $\frac{\Delta t}{2}\omega_0$  $\mathbf{r}_i$  $\mathbf{r}_{i+1}$ 

$$\Delta t \|\mathbf{v}_{i+1/2}\| = \Delta t r \omega$$

 $\mathbf{r}(t_{i+1})$  $\underbrace{\hspace{10em}}$